

# Recent developments in the holographic description of quantum chaos.

Viktor Jahnke<sup>a,b</sup>

<sup>a</sup>*Departamento de Física de Altas Energias, Instituto de Ciencias Nucleares,  
Universidad Nacional Autónoma de México  
Apartado Postal 70-543, CDMX 04510, México*

<sup>b</sup>*School of Physics and Chemistry, Gwangju Institute of Science and Technology,  
Gwangju 61005, Korea*

`viktor.jahnke@correo.nucleares.unam.mx`  
`viktorjahnke@gist.ac.kr`

## Abstract

We review recent developments encompassing the description of quantum chaos in holography. We discuss the characterization of quantum chaos based on the late time vanishing of out-of-time-order correlators and explain how this is realized in the dual gravitational description. We also review the connections of chaos with spreading of quantum entanglement and diffusion phenomena.

# Contents

<b>1</b>	<b>Introduction</b>	<b>1</b>
<b>2</b>	<b>A bird eye's view on classical chaos</b>	<b>2</b>
<b>3</b>	<b>Some aspects of quantum chaos</b>	<b>4</b>
3.1	Operator growth and scrambling . . . . .	9
3.2	Probing chaos with local operators . . . . .	10
<b>4</b>	<b>Chaos &amp; Holography</b>	<b>11</b>
4.1	Holographic setup . . . . .	13
4.2	Bulk picture for the behaviour of OTOCs . . . . .	18
4.2.1	Stringy corrections . . . . .	22
4.2.2	Bounds on chaos . . . . .	24
4.3	Chaos and Spreading of Entanglement . . . . .	25
4.4	Chaos & Hydrodynamics . . . . .	28
<b>5</b>	<b>Closing remarks</b>	<b>29</b>

## 1 Introduction

The characterization of quantum chaos is fairly complicated. Possible approaches range from semi-classical methods to random matrix theory: in the first case one studies the semi-classical limit of a system whose classical dynamics is chaotic; in the later approach the characterization of quantum chaos is made by comparing the spectrum of energies of the system in question to the spectrum of random matrices [1]. Despite the insights provided by aforementioned approaches a complete and more satisfactory understanding of quantum chaos remains elusive.

Surprisingly, new insights into quantum chaos have come from black holes physics! In the context of so-called gauge gravity duality [2–4], black holes in asymptotically AdS spaces are dual to strongly coupled many-body quantum systems. It was recently shown that the chaotic nature of many-body quantum systems can be diagnosed with certain out-of-time-order correlation (OTOC) functions which, in the gravitational description, are related to the collision of shock waves close to the black hole horizon [5–9]. In

addition to being useful for diagnosing chaos in holographic systems and providing a deeper understanding for the inner-working mechanisms of gauge-gravity duality, OTOCs have also proved useful in characterizing chaos in more general non-holographic systems, including some simple models like the kicked-rotor [10], the stadium billiard [11], and the Dicke model [12].

In this paper we review the recent developments in the holographic description of quantum chaos. We discuss the characterization of quantum chaos based on the late time vanishing of OTOCs and explain how this is realized in the dual gravitational description. We also review the connections of chaos with spreading of quantum entanglement and diffusion phenomena. We focus on the case of  $d$ -dimensional gravitational systems with  $d \geq 3$ , which excludes the case of gravity in  $AdS_2$  and SYK-like models [13–16]<sup>1</sup>. Also, due the lack of the author expertise, we did not cover the recent developments in the direct field theory calculations of OTOCs. This includes calculations for CFTs [20], weakly coupled systems [21, 22], random unitary models [23–25] and spin chains [26–30].

## 2 A bird eye's view on classical chaos

In this section we briefly review some basic aspects of classical chaos. For definiteness we consider the case of a classical thermal system with phase space denoted as  $\mathbf{X} = (\mathbf{q}, \mathbf{p})$ , where  $\mathbf{q}$  and  $\mathbf{p}$  are multi-dimensional vectors denoting the coordinates and momenta of the phase space. We can quantify whether the system is chaotic or not by measuring the stability of a trajectory in phase space under small changes of the initial condition. Let us consider a reference trajectory in phase space  $\mathbf{X}(t)$ , with some initial condition  $\mathbf{X}(0) = \mathbf{X}_0$ . A small change in the initial condition  $\mathbf{X}_0 \rightarrow \mathbf{X}_0 + \delta\mathbf{X}_0$  leads to a new trajectory  $\mathbf{X}(t) \rightarrow \mathbf{X}(t) + \delta\mathbf{X}(t)$ . This is illustrated in figure 1. For a chaotic system, the distance between the new trajectory and the reference one increases exponentially with time

$$|\delta\mathbf{X}(t)| \sim |\delta\mathbf{X}_0| e^{\lambda t} \quad \text{or} \quad \frac{\partial \mathbf{X}(t)}{\partial \mathbf{X}_0} \sim e^{\lambda t}, \quad (1)$$

where  $\lambda$  is the so-called Lyapunov exponent. This should be contrasted with the behaviour of non-chaotic systems, in which  $\delta\mathbf{X}(t)$  remains bounded or increase algebraically [31].

The exponential increase depends on the orientation of  $\delta\mathbf{X}_0$  and this leads to a spectrum of Lyapunov exponents,  $\{\lambda_1, \lambda_2, \dots, \lambda_K\}$ , where  $K$  is the dimensionality of the

---

<sup>1</sup>Another interesting perspective on the characterization of chaos in the context of (regularized)  $AdS_2/CFT_1$  is provided by [17–19].

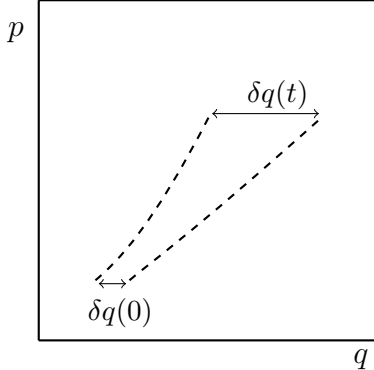


Figure 1: Variation of a trajectory in the phase space under small modifications of the initial condition. For a chaotic system the distance between two initially nearby trajectories increases exponentially with time, i.e.,  $|\delta q(t)| = |\delta q(0)|e^{\lambda t}$ .

phase space. A useful parameter characterizing the trajectory instability is

$$\lambda_{\max} = \lim_{t \rightarrow \infty} \lim_{\delta \mathbf{X}_0 \rightarrow 0} \frac{1}{t} \log \left( \frac{\delta \mathbf{X}(t)}{\delta \mathbf{X}_0} \right), \quad (2)$$

which is called the maximum Lyapunov exponent. When the above limits exist and  $\lambda_{\max} > 0$  the trajectory shows sensitive to initial conditions and the system is said to be chaotic [31].

The chaotic behaviour can be either a consequence of a complicated Hamiltonian or simply due to the contact with a thermal heat bath. This is because chaos is a common property of thermal systems. To later to make contact with black holes physics we consider the case of a classical thermal system with inverse temperature  $\beta$ . If  $F(\mathbf{X})$  is some function of the phase space coordinates we define its classical expectation value as

$$\langle F \rangle_{\beta} = \frac{\int d\mathbf{X} e^{-\beta H(\mathbf{X})} F(\mathbf{X})}{\int d\mathbf{X} e^{-\beta H(\mathbf{X})}} \quad (3)$$

where  $H(\mathbf{X})$  is the system's Hamiltonian.

Classical thermal systems have two exponential behaviours that have analogues in terms of black holes physics: the Lyapunov behaviour, characterizing the sensitive dependence on initial conditions; and the Ruelle behaviour, characterizing the approach to thermal equilibrium [32].

To quantify the sensitive to initial conditions in a thermal system we need to consider thermal expectation values. Note that (1) can have either signs. To avoid cancellations in a thermal expectation values we consider the square of this derivative

$$F(t) = \left\langle \left( \frac{\partial \mathbf{X}(t)}{\partial \mathbf{X}(0)} \right)^2 \right\rangle_{\beta}. \quad (4)$$

The expected behaviour of this quantity is the following [33]

$$F(t) \sim \sum_k c_k e^{2\lambda_k t}, \quad (5)$$

where  $c_k$  are constants and  $\lambda_k$  are the Lyapunov exponents. At later times the behaviour is controlled by the maximum Lyapunov exponent  $F \sim e^{2\lambda_{\max} t}$ .

The approach to thermal equilibrium or, in other words, how fast the system forgets its initial condition, can be quantified by two-point functions of the form

$$G(t) = \langle \mathbf{X}(t) \mathbf{X}(0) \rangle_\beta - \langle \mathbf{X} \rangle_\beta^2, \quad (6)$$

whose expected behaviour is [33]

$$G(t) \sim \sum_j b_j e^{-\mu_j t}, \quad (7)$$

where  $b_j$  are constants and  $\mu_j$  are complex parameters called the Ruelle resonances. The late time behaviour is controlled by the smallest Ruelle resonance  $G \sim e^{-\mu_{\min} t}$ .

### 3 Some aspects of quantum chaos

In this section we review some aspects of quantum chaos. For a long time, the characterization of quantum chaos was made by comparing the spectrum of energies of the system in question to the spectrum of random matrices or using semiclassical methods [1]. Here we follow a different approach, which was first proposed by Larkin and Ovchinnikov [34] in the context of semi-classical systems, and it was recently developed by Shenker and Stanford [6–8] and by Kitaev [9].

For simplicity, let us consider the case of a one-dimensional system, with phase space variables  $(q, p)$ . Classically, we know that  $\partial q(t)/\partial q(0)$  grows exponentially with time for a chaotic system. The quantum version of this quantity can be obtained by noting that

$$\frac{\partial q(t)}{\partial q(0)} = \{q(t), p(0)\}_{\text{P.B.}}, \quad (8)$$

where  $\{q(t), p(0)\}_{\text{P.B.}}$  denotes the Poisson bracket between the coordinate  $q(t)$  and the momentum  $p(0)$ . The quantum version of  $\partial q(t)/\partial q(0)$  can then be obtained by promoting the Poisson bracket to a commutator

$$\{q(t), p(0)\}_{\text{P.B.}} \rightarrow \frac{1}{i\hbar} [\hat{q}(t), \hat{p}(0)] \quad (9)$$

where now  $\hat{q}(t)$  and  $\hat{p}(0)$  are Heisenberg operators.

We will be interested in thermal systems, so we would like to calculate the expectation value of  $[\hat{q}(t), \hat{p}(0)]$  in a thermal state. However, this commutator might have either signs in a thermal expectation value and this might lead to cancellations. To overcome this problem, we consider the expectation value of the square of this commutator

$$C(t) = \langle -[\hat{q}(t), \hat{p}(0)]^2 \rangle_\beta, \quad (10)$$

where  $\beta$  is the system's inverse temperature and the overall sign is introduced to make  $C(t)$  positive. More generally, one might replace  $\hat{q}(t)$  and  $\hat{p}(0)$  by two generic hermitian operators  $V$  and  $W$  and quantify chaos with the *double commutator*

$$C(t) = \langle -[W(t), V(0)]^2 \rangle_\beta. \quad (11)$$

This quantity measures how much an early perturbation  $V$  affects the later measurement of  $W$ . As chaos means sensitive dependence on initial conditions, we expect  $C(t)$  to be ‘small’ in non-chaotic system, and ‘large’ when there is chaos. In the following we give a precise meaning for the adjectives ‘small’ and ‘large’.

For some class of systems the quantum behaviour of  $C(t)$  has a lot of similarities with the classical behavior of  $\langle (\partial q(t)/\partial q(0)) \rangle_\beta$ . The analogy between the classical and quantum quantities is not perfect because there is not always a good notion of a small perturbation in the quantum case (remember that classical chaos is characterized by the fact that a small perturbation in the past have important consequences in the future). If we start with some reference state and then perturb it, we easily produce a state that is orthogonal to the original state, even when we change just a few quantum numbers. Because of that it seems unnatural to quantify the perturbation as small. Fortunately, there are some quantum systems in which the notion of a small perturbation makes perfect sense. An example is provided by systems with a large number of degrees of freedom. In this case a perturbation involving just a few degrees of freedom is naturally a small perturbation.

For some class of chaotic systems, which include holographic systems,  $C(t)$  is expected to behave as<sup>2</sup>

$$C(t) \sim \begin{cases} N_{\text{dof}}^{-1} & \text{for } t < t_d, \\ N_{\text{dof}}^{-1} \exp(\lambda_L t) & \text{for } t_d \ll t \ll t_*, \\ \mathcal{O}(1) & \text{for } t > t_*, \end{cases}$$

where  $N_{\text{dof}}$  is the number of degrees of freedom of the system. Here, we have assumed  $V$  and  $W$  to be unitary and hermitian operators, so that  $VV = WW = 1$ . The expo-

---

<sup>2</sup>See [30, 35] for a discussion of different possible OTOC growth forms.

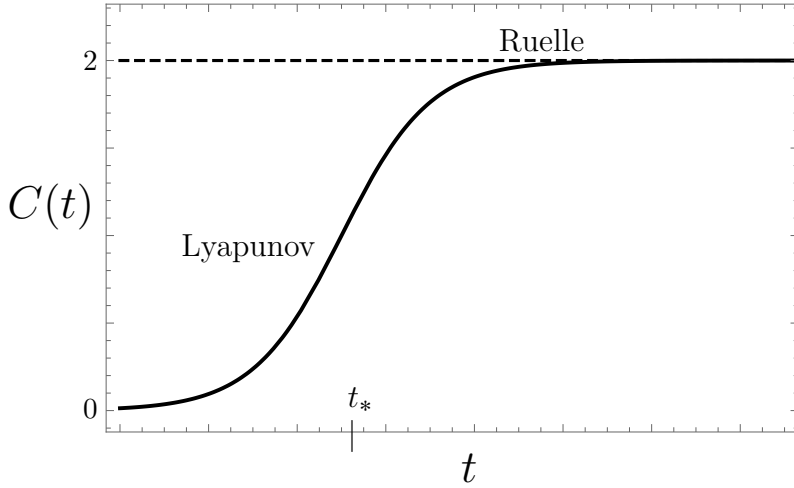


Figure 2: Schematic form of  $C(t)$ . We indicated the regions of Lyapunov and Ruelle behaviour.  $C(t) \sim \mathcal{O}(1)$  at  $t \sim t_*$ .

ential growth of  $C(t)$  is characterized by the Lyapunov exponent<sup>3</sup>  $\lambda_L$  and takes place at intermediate time scales bounded by the dissipation time  $t_d$  and the scrambling time  $t_*$ . The dissipation time is related to the classical Ruelle resonances ( $t_d \sim \mu^{-1}$ ) and it characterizes the exponential decay of two-point correlators, e.g.,  $\langle V(0)V(t) \rangle \sim e^{-t/t_d}$ . The dissipation time also controls the late time behaviour of  $C(t)$ . The scrambling time  $t_* \sim \lambda_L^{-1} \log N_{\text{dof}}$  is defined as the time at which  $C(t)$  becomes of order  $\mathcal{O}(1)$ . See figure 2. The scrambling time controls how fast the chaotic system scrambles information. If we perturb the system with an operator that involves only a few degrees of freedom, the information about this operator will spread among the other degrees of freedom of the system. After a scrambling time, the information will be scrambled among all the degrees of freedom and the operator will have a large commutator with almost any other operator.

To understand how the above behaviour relates to chaos, we write the double commutator as

$$C(t) = \langle -[W(t), V(0)]^2 \rangle_\beta \quad (12)$$

$$= 2 - 2 \text{Re}(\langle W(t)V(0)W(t)V(0) \rangle_\beta), \quad (13)$$

where we made the assumption that  $W$  and  $V$  are hermitian operators. Note that all the relevant information about  $C(t)$  is contained in the OTOC

$$\text{OTOC}(t) = \langle W(t)V(0)W(t)V(0) \rangle. \quad (14)$$

---

<sup>3</sup>This is actually the quantum analogue of the classical Lyapunov exponent. The two quantities are not necessarily the same in the classical limit [21]. Here we stick to the physicists long standing tradition of using misnomers and just refer to  $\lambda_L$  as the Lyapunov exponent.

The fact that  $C(t)$  approaches 2 at later times implies that the  $\text{OTO}(t)$  should vanish in that limit. To understand why this is related to chaos we think of  $\text{OTO}(t)$  as an inner-product of two states

$$\text{OTO}(t) = \langle \psi_2 | \psi_1 \rangle, \quad (15)$$

where

$$|\psi_1\rangle = W(-t)V(0)|\beta\rangle, \quad |\psi_2\rangle = V(0)W(-t)|\beta\rangle \quad (16)$$

where  $|\beta\rangle$  is some thermal state and we replace  $t \rightarrow -t$  to make easier the comparison with black holes physics.

If  $[V(0), W(t)] \approx 0$  for any value of  $t$ , the two states are approximately the same, and  $\langle \psi_1 | \psi_2 \rangle \approx 1$ , implying  $C(t) \approx 0$ . That means the system displays no chaos - the early measurement of  $V$  has no effect on the later measurement of  $W$ . If, on the other hand,  $[V(0), W(t)] \neq 0$ , the states  $|\psi_1\rangle$  and  $|\psi_2\rangle$  will have a small superposition  $\langle \psi_1 | \psi_2 \rangle \approx 0$ , implying  $C(t) \approx 2$ . That means that  $V$  has a large effect on the later measurement of  $W$ .

In figure 3 we construct the states  $|\psi_1\rangle$  and  $|\psi_2\rangle$  and explain why  $\langle \psi_1 | \psi_2 \rangle \approx 0$  for large  $t$  means chaos. Let us start by constructing the state  $|\psi_1\rangle = W(-t)V(0)|\beta\rangle = e^{-iHt}W(0)e^{iHt}V(0)|\beta\rangle$ . The unperturbed thermal state is represented by a horizontal line. We initially consider the state  $V(0)|\beta\rangle$ , which is the thermal state perturb by  $V$ . If we evolve the system backwards in time (applying the operator  $e^{iHt}$ ) for some time which is larger than the dissipation time, the system will thermalize and it will no longer displays the perturbation  $V$ . After that, we apply the operator  $W$ , which should be thought of as a small perturbation, and then we evolve the system forwards in time (applying the operator  $e^{-iHt}$ ). The final results of this set of operations depends on the nature of the system. If the system is chaotic, the perturbation  $W$  will have a large effect after a scrambling time, and the perturbation that was present at  $t = 0$  will no longer re-materialize. This is illustrated in figure 3. In contrast, for a non-chaotic system, the perturbation  $W$  will have little effect on the system at later times, and the perturbation  $V$  will (at least partially) re-materialize at  $t = 0$ .

We now construct the state  $|\psi_2\rangle = V(0)W(-t)|\beta\rangle = V(0)e^{-iHt}W(0)e^{iHt}|\beta\rangle$ . This is illustrated in figure 4. We start with the thermal state  $|\beta\rangle$  and then we evolve this state backwards in time  $e^{iHt}|\beta\rangle$ . After that we apply the operator  $W$  and then we evolve the system forwards in time, obtaining the state  $e^{-iHt}W(0)e^{iHt}|\beta\rangle$ . Finally, we apply the operator  $V$ , obtaining the state  $V(0)W(-t)|\beta\rangle$ . Note that, by construction, this state displays the perturbation  $V$  at  $t = 0$ , while the state  $W(-t)V(0)|\beta\rangle$  does not. As a consequence, the two states are expected to have a small superposition  $\langle W(-t)V(0) | W(-t)V(0) \rangle_\beta \approx 0$ . This should be contrasted to the case where the system is not chaotic. In this case the perturbation  $V$  re-materializes at  $t = 0$ , and the states  $|\psi_1\rangle$  and  $|\psi_2\rangle$  have a large superposition, i.e.,  $\langle W(-t)V(0) | W(-t)V(0) \rangle_\beta \approx 1$ .

In this construction we assumed the operators  $V(0)$  and  $W(-t)$  to be separated by a scrambling time, i.e.,  $|t| > t_*$ . This is important because, at earlier times, the two operators, which generically involve different degrees of freedom of the system, generically commute. The operators manage to have a non-zero commutator at later times because of the phenomenon of operation growth that we will describe in the next section.

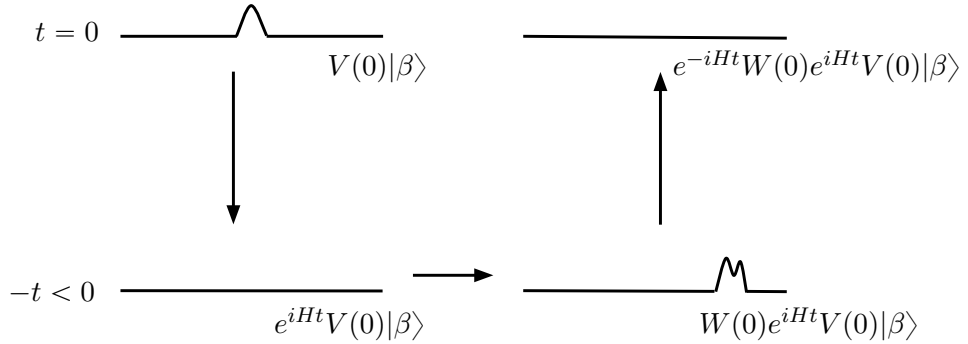


Figure 3: Construction of the state  $W(-t)V(0)|\beta\rangle$ . For a chaotic system the perturbation  $V$  fails to re-materialize at  $t = 0$ . In a non-chaotic system we expect the perturbation  $V$  to re-materialize at  $t = 0$ .

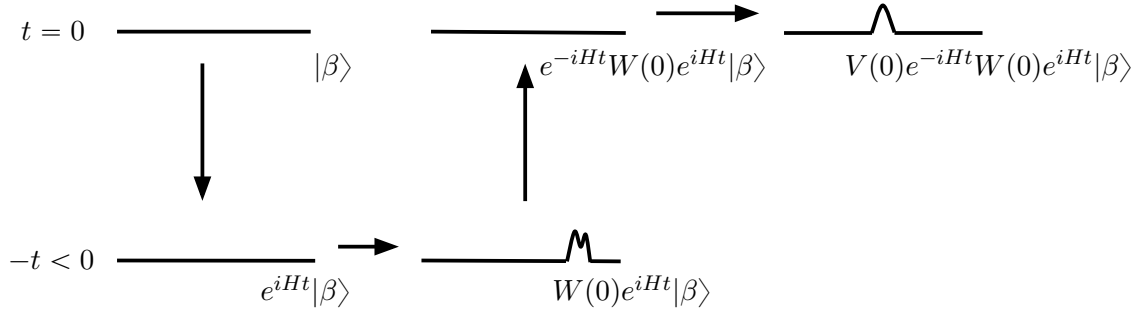


Figure 4: Construction of the state  $V(0)W(-t)|\beta\rangle$ . By construction, this state displays the perturbation  $V$  at  $t = 0$ .

### 3.1 Operator growth and scrambling

The operators  $V$  and  $W$  act generically at different parts of the physical system, yet they can have a non-zero commutator at later times. This is possible because in chaotic systems the time evolution of an operator makes it more and more complicated, involving and increasing number of degrees of freedom. As a result, an operator that initially involves just a few degrees of freedom, becomes delocalized over a region that grows with time. The growth of the operator  $W(t)$  is maybe more evident from the point of view of the Baker-Campbell-Hausdorff (BCH) formula, in terms of which we can write

$$W(t) = e^{iHt}W(0)e^{-iHt} = \sum_{k=0}^{\infty} \frac{(-it)^k}{k!} [H[H, \dots [H, W(0)] \dots]]. \quad (17)$$

From the above formula it is clear that, at each order in  $t$  there is a more complicated contribution to  $W(t)$ . In chaotic systems the operator becomes more and more delocalized as the time evolves, and it eventually becomes delocalized over the entire system. The time scale at which this occurs is the so-called scrambling time  $t_*$ . After the scrambling time the operator  $W(t)$  manages to have a non-zero and large commutator with almost any other operator, even operators involving only a few degrees of freedom.

This can be clearly illustrated in the case of a spin-chain. Let us follow [7] and consider an Ising-like model with Hamiltonian

$$H = - \sum_i (Z_i Z_{i+1} + g X_i + h Z_i), \quad (18)$$

where  $X_i, Y_i$  and  $Z_i$  denote Pauli matrices acting on the  $i$ th site of the spin chain. The above system is integrable if we take  $g = 1$  and  $h = 0$ , but it is strongly chaotic if we choose  $g = -1.05$  and  $h = 0.5$ .

To illustrate the concept of scrambling, we consider the time evolution of the operator  $Z_1$ . Using the BCH formula we can write

$$Z_1(t) = Z_1 - it[H, Z_1] - \frac{t^2}{2!}[H, [H, Z_1]] + \frac{it^3}{3!}[H, [H, [H, Z_1]]] + \dots \quad (19)$$

Ignoring multiplicative constants and signs we can write the above terms (schematically) as

$$\begin{aligned}
[H, Z_1] &\sim Y_1 & (20) \\
[H, [H, Z_1]] &\sim Y_1 + X_1 Z_2 \\
[H, [H, [H, Z_1]]] &\sim Y_1 + Y_2 X_1 + Y_1 Z_2 \\
[H, [H, [H, [H, Z_1]]]] &\sim X_1 + Y_1 + Z_1 + X_1 X_2 + Y_1 Y_2 + Z_1 Z_2 + X_1 Z_2 + \\
&\quad + Z_3 Y_1 + Y_1 Z_2 Y_2 + Z_1 X_2 X_1 + X_2 Z_3 X_1
\end{aligned}$$

As the time evolves higher order terms become important in the series (19), and the operator  $Z_1(t)$  becomes more and more complicated, involving terms in an increasing number of sites. For large enough  $t$  the operator will involve all the sites of the spin chain and it will manage to have a non-zero commutator with a Pauli operator in any other site of the system. In this situation the information about  $Z_1$  is essentially scramble among all the degrees of freedom of the system. As discussed before, this occurs after a scrambling time. Above this time the double commutator  $C(t)$  saturates to a constant value. This should be contrasted to what happens for an integrable system. In this case the operator grows, but it also decreases at later times. In the chaotic case, the operator remains large at later times [7].

### 3.2 Probing chaos with local operators

In quantum field theories we can upgrade (11) to the case where the operators are separated in space

$$C(t, x) = \langle -[V(0, 0), W(t, x)]^2 \rangle_\beta. \quad (21)$$

Strictly speaking, the above expression is generically divergent, but it can be regularized by adding imaginary times to the time arguments of the operators  $V$  and  $W$ . For a large class of spin-chains, higher dimensional SYK-models and CFTs the above commutator is roughly given by

$$C(t, x) \sim \exp \left[ \lambda_L \left( t - t_* - \frac{|x|}{v_B} \right) \right], \quad (22)$$

where  $v_B$  is the so-called butterfly velocity<sup>4</sup>. This velocity describes the growth of the operator  $W$  in physical space and it acts as a low-energy Lieb-Robinson velocity [36], which sets a bound for the rate of transfer of quantum information. From the above formula, we can see that there is an additional delay in scrambling due to the physical separation between the operators. The butterfly velocity defines an effective light-cone for the commutator (21). Inside the cone, for  $t - t_* \geq |x|/v_B$ , we have

---

<sup>4</sup>Actually,  $v_B$  represents the “velocity of the butterfly effect”. Here we continue to follow the tradition of using misnomers.

$C(t, x) \sim \mathcal{O}(1)$ , whereas for outside the cone, for  $t - t_* < |x|/v_B$ , the commutator is small,  $C(t, x) \sim 1/N_{\text{dof}} \ll 1$ . Outside the light-cone the Lorentz invariance implies a zero commutator. The light-cone and the butterfly effect cone are illustrated in figure 5.

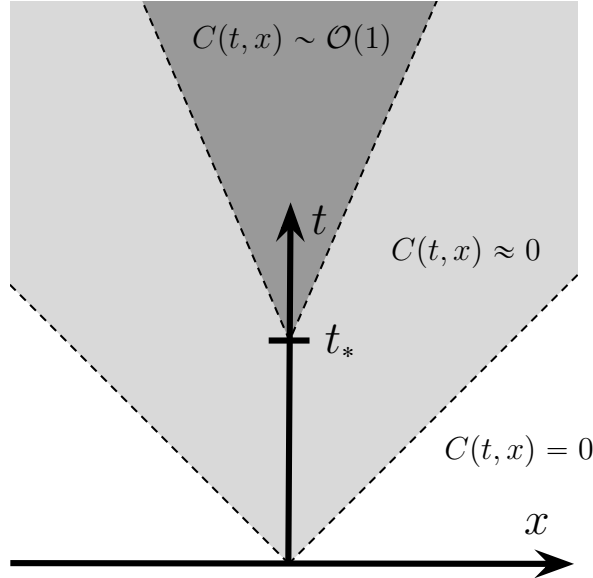


Figure 5: Light cone (gray region) and butterfly effect cone (dark gray region). Inside the butterfly effect cone, for  $t - t_* \geq |x|/v_B$ , we have  $C(t, x) \sim \mathcal{O}(1)$ , whereas for outside the cone, for  $t - t_* < |x|/v_B$ , the commutator is small,  $C(t, x) \sim 1/N_{\text{dof}} \ll 1$ . Outside the light-cone the Lorentz invariance implies a zero commutator.

## 4 Chaos & Holography

In this section we review how the chaotic properties of holographic theories can be described in terms of black holes physics. Black holes behave as thermal systems and thermal systems generically display chaos. This implies that black holes are somehow chaotic. This statement has a precise realization in the context of the gauge/gravity duality. According to this duality, some strongly coupled non-gravitational systems are dual to higher dimensional gravitational systems. In the most known and studied example of this duality the  $\mathcal{N} = 4$  super Yang-Mills (SYM) theory living in  $R^{3,1}$  is dual to type IIB supergravity in  $AdS_5 \times S^5$ . More generically, a  $d$ -dimensional non-gravitational theory living in  $R^{d-1,1}$  is dual to a gravity theory living in a higher-dimensional space of the form  $AdS_{d+1} \times \mathcal{M}$ , where  $\mathcal{M}$  is generically a compact manifold. The non-gravitational theory can be thought as living in the boundary of  $AdS_{d+1}$  and

because of that is usually called the *boundary theory*. The gravitational theory is also called the *bulk theory*.

There is a dictionary relating physical quantities in the boundary and bulk description [3, 4]. An example is provided by the operators of the boundary theory that are related to bulk fields. The boundary theory at finite temperature can be described by introducing a black hole in the bulk. The thermalization properties of the boundary theory have a nice visualization in terms of black holes physics. By applying a local operator in the boundary theory we produce some perturbation that describes a small deviation from the thermal equilibrium. The information about  $V(x)$  is initially contained around the point  $x$ , but it gets delocalized over a region that increases with time, until it completely melts into the thermal bath. In the bulk theory, the application of the operator  $V(x)$  produces a particle (field excitation) close to the boundary of the space, which then falls into the black hole. The return to the thermal equilibrium in the boundary theory corresponds to the absorption of the bulk particle by the black hole. Figure 6 illustrates this bulk description of thermalization.

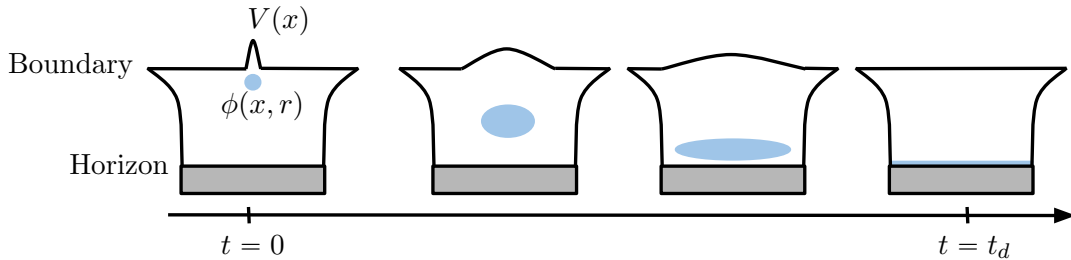


Figure 6: Bulk picture of thermalization. The figure represents an asymptotically *AdS* black hole geometry. The boundary is at the top edge, while the black hole horizon is at the bottom edge. The black hole's interior is shown in gray. The boundary operator  $V$  is dual to the bulk field  $\phi$ . From the point of view of the boundary theory the perturbation produced by  $V$  is initially localized around the point  $x$ , but it gets delocalized over a region that increases with time. In the bulk description this is described by a particle (field excitation) that is initially close to the boundary and then falls into the black hole.

The approach to thermal equilibrium is controlled by the black hole's quasi-normal modes (QNMs). In holographic theories, the quasi-normal modes control the decay of two-point functions of the boundary theory

$$\langle V(t)V(0) \rangle_\beta \sim e^{-t/t_d} \quad (23)$$

where the dissipation time  $t_d$  is related to the lowest quasi-normal mode ( $\text{Im}(\omega) \sim t_d^{-1}$ ). From the point of view of the bulk theory the QNMs describes how fast a perturbed

black hole returns to equilibrium. Clearly, the black hole's quasi-normal modes correspond to the classical Ruelle resonances. In holographic theories the dissipation time is roughly give by  $t_d \sim \beta$ .

Another important exponential behaviour of black holes is provided by the blue shift suffered by the in-falling quanta, or, equivalently, the red shift suffered by the quanta escaping from the black hole. The blue-shift suffered by the in-falling quanta is determined by the black hole's temperature. If the quanta asymptotic energy is  $E_0$ , this energy increases exponentially with time

$$E = E_0 e^{\frac{2\pi}{\beta} t}, \quad (24)$$

where  $\beta$  is the Hawking's inverse temperature. Later we will see that this exponential increase in the energy of the in-falling quanta gives rise to the Lyapunov behaviour of  $C(t, x)$  of holographic theories.

## 4.1 Holographic setup

### The TFD state & Two-sided black holes

In the study of chaos is convenient to consider a thermofield double state made out of two identical copies of the boundary theory

$$|\text{TFD}\rangle = \frac{1}{Z^{1/2}} \sum_n e^{-\beta E_n/2} |n\rangle_L |n\rangle_R, \quad (25)$$

where  $L$  and  $R$  label the states of the two copies, which we call  $\text{QFT}_L$  and  $\text{QFT}_R$ , respectively. The two boundary theories do not interact, and only know about each other through their entanglement. This state is dual to a eternal (two-sided) black hole, with two asymptotic boundaries, where the boundary theories live [37]. This is a wormhole geometry, with an Einstein-Rosen bridge connecting the two sides of the geometry. The wormhole is not traversable, which is consistent with the fact that the two boundary theories do not interact.

For definiteness we assume a metric of the form

$$ds^2 = -G_{tt}(r)dt^2 + G_{rr}(r)dr^2 + G_{ij}(r, x^k)dx^i dx^j, \quad (26)$$

where the boundary is located at  $r = \infty$ , where the above metric is assumed to asymptote  $AdS_{d+1}$ . We take the horizon as located at  $r = r_H$ , where  $G_{tt}$  vanish and  $G_{rr}$  has a first order pole. For future purposes, let  $\beta$  be the Hawking's inverse temperature, and  $S_{\text{BH}}$  be the Bekenstein-Hawking entropy.

In the study of shock waves is more convenient to work with Kruskal-Szekeres coordinates, since these coordinate cover smoothly the globally extended spacetime. We first define the tortoise coordinate

$$dr_* = \sqrt{\frac{G_{rr}}{G_{tt}}} dr, \quad (27)$$

and then we introduce the Kruskal-Szekeres coordinates  $U, V$  as

$$\begin{aligned} U &= +e^{\frac{2\pi}{\beta}(r_*-t)}, \quad V = -e^{\frac{2\pi}{\beta}(r_*+t)} \quad (\text{left exterior region}) \\ U &= -e^{\frac{2\pi}{\beta}(r_*-t)}, \quad V = +e^{\frac{2\pi}{\beta}(r_*+t)} \quad (\text{right exterior region}) \\ U &= +e^{\frac{2\pi}{\beta}(r_*-t)}, \quad V = +e^{\frac{2\pi}{\beta}(r_*+t)} \quad (\text{future interior region}) \\ U &= -e^{\frac{2\pi}{\beta}(r_*-t)}, \quad V = -e^{\frac{2\pi}{\beta}(r_*+t)} \quad (\text{past interior region}) \end{aligned} \quad (28)$$

In terms of these coordinates the metric reads

$$ds^2 = 2A(UV)dUdV + G_{ij}(UV)dx^i dx^j, \quad (29)$$

where

$$A(UV) = \frac{\beta^2}{8\pi^2} \frac{G_{tt}(UV)}{UV}. \quad (30)$$

In these coordinates the horizon is located at  $U = 0$  or at  $V = 0$ . The boundary (left or right) is located at  $UV = -1$  and the singularity at  $UV = 1$ . The Penrose diagram for this metric is shown in figure 7.

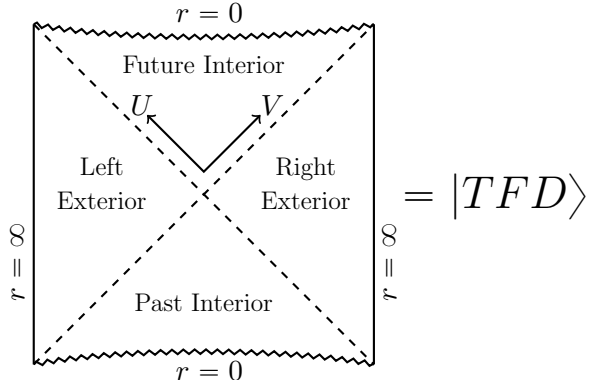


Figure 7: Penrose diagram for the two-sided black holes with two boundaries that asymptote  $AdS$ . This geometry is dual a thermofield double state constructed out of two copies of the boundary theory.

The global extended spacetime can also be described in terms of complexified coordinates [38]. In this case one defines the complexified Schwarzschild time

$$t = t_L + i t_E, \quad (31)$$

where  $t_L$  and  $t_E$  are the Lorentzian and Euclidean times, and then one describes the time in each of the four patches (left and right exterior regions, and the future and past interior regions) as having a constant imaginary part

$$\begin{aligned} t_E &= 0 & (\text{right exterior region}) \\ t_E &= -\beta/4 & (\text{future interior region}) \\ t_E &= -\beta/2 & (\text{left exterior region}) \\ t_E &= +\beta/4 & (\text{past interior region}) \end{aligned} \tag{32}$$

The Euclidean time has a period of  $\beta$ . The Lorentzian time increases upward (downward) in the right (left) exterior region, and to the right (left) in the future (past) interior.

Note that, with the complexified time, one can obtain an operator acting on the left boundary theory by adding (or subtracting)  $i\beta/2$  to the time of an operator acting on the right boundary theory.

### Perturbations of the TFD state & Shock wave geometries

We now turn to the description of states of the form

$$W(t)|TFD\rangle \tag{33}$$

where  $W_R$  is a thermal scale operator that acts on the right boundary theory. This state can be described by a ‘particle’ (field excitation) in the bulk that comes out of the past horizon, reaches the right boundary at time  $t$ , and then falls into the future horizon, as illustrated in figure 8.

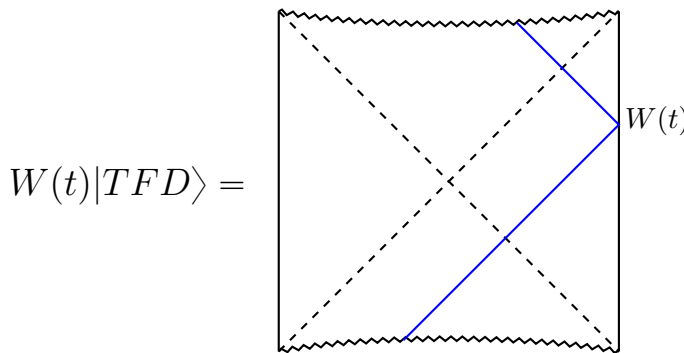


Figure 8: Bulk description of the state  $W(t)|TFD\rangle$ . In blue is shown the trajectory of a ‘particle’ that comes out of the past horizon, reaches the boundary at time  $t$  producing the perturbation  $W$ , and then falls into the future horizon.

If  $|t|$  is not too large, the state  $W(t)|\text{TFD}\rangle$  will represent just a small perturbation of the TFD state and the corresponding description in the bulk will be just an eternal two-sided black hole geometry slightly perturbed by the presence of a probe particle. This is no longer the case if  $|t|$  is large. In this case there is a non-trivial modification of the geometry. A very early perturbation, for example, is described in the bulk in terms of a particle that falls towards the future horizon for a very long time and gets highly blue shifted in the process. If the particle's energy is  $E_0$  in the asymptotic past, this energy will be exponentially larger from the point of view of the  $t = 0$  slice of the geometry, i.e.,  $E = E_0 e^{\frac{2\pi}{\beta}t}$ . Therefore, for large enough  $|t|$ , the particle's energy will be very large and one needs to include the corresponding back-reaction.

The back-reaction of a very early (or very late) perturbation is actually very simple - it corresponds to a shock wave geometry [39, 40]. To understand that, we first need to notice that, under boundary time evolution, the stress energy of a generic perturbation  $W_R$  gets compressed in the  $V$ -direction, and stretched in the  $U$ -direction. For large enough  $|t|$  we can approximate the stress tensor of the W-particle as

$$T_{VV} \sim P^U \delta(V) a(\vec{x}), \quad (34)$$

where  $P^U \sim \beta^{-1} e^{\frac{2\pi}{\beta}t}$  is the momentum of the W-particle in the  $U$ -direction and  $a(\vec{x})$  is some generic function that specifies the location of the perturbation in the spatial directions of the right boundary. Note that  $T_{VV}$  is completely localized at  $V = 0$ , and homogeneous along the  $U$ -direction. Besides that, even if the W-particle is massive, the exponential blue-shift will make it follow an almost null trajectory, as shown in figure 9.

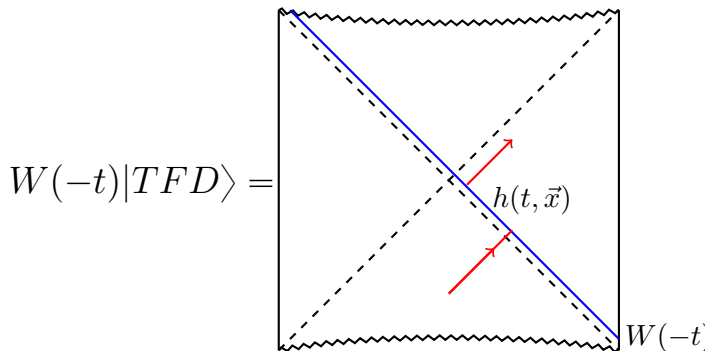


Figure 9: Bulk description of the state  $W(-t)|\text{TFD}\rangle$ . An early enough perturbation produces a shock wave geometry. The effect of the shock wave (shown in blue) is to produce a shift  $U \rightarrow U + h(x)$  in the trajectory of a probe particle (shown in red) crossing it.

The shock wave geometry produced by the W-particle is described by the metric

$$ds^2 = 2A(UV)dUdV + G_{ij}(UV)dx^i dx^j - 2A(UV)h(t, \vec{x})\delta(V)dV^2, \quad (35)$$

that is completely specified by the shock wave transverse profile  $h(t, \vec{x})$ . This geometry can be seen as two pieces of a eternal black hole glued together along  $V = 0$  with a shift of magnitude  $h(t, \vec{x})$  in the  $U$ -direction. We find useful to represent this geometry with the same Penrose diagram of the unperturbed geometry, but with the prescription that any trajectory crossing the shock wave gets shifted in the  $U$ -direction as  $U \rightarrow U + h(t, \vec{x})$ . See figure 9.

The precise form of  $h(t, \vec{x})$  can be determined by solving the  $VV$ -component of Einstein's equation. For a local perturbation, i.e.,  $a(\vec{x}) = \delta^{d-1}(\vec{x})$ , the solution reads

$$h(t, \vec{x}) \sim G_N e^{\frac{2\pi}{\beta}t - \mu|\vec{x}|}, \quad \text{with } \mu = \frac{2\pi}{\beta} \sqrt{\frac{(d-1)G'_{ii}(r_H)}{G'_{tt}(r_H)}}, \quad (36)$$

where, for simplicity,  $G_{ij}$  has been assumed to be diagonal and isotropic.

Interestingly, the shock wave profile contains information about the parameters characterizing the chaotic behaviour of the boundary theory. Indeed, the double commutator has a region of exponential growth at which  $C(t, \vec{x}) \sim h(t, \vec{x})$ . From this identification, we can write

$$h(t, \vec{x}) \sim \frac{1}{N_{\text{dof}}} e^{\frac{2\pi}{\beta}(t - t_* - \frac{|\vec{x}|}{v_B})} \quad (37)$$

where  $N_{\text{dof}} \sim 1/G_N$ , and the leading order contribution to the scrambling time scales logarithmically with the Bekenstein-Hawking entropy

$$t_* \sim \frac{\beta}{2\pi} \log \frac{1}{G_N} \sim \frac{\beta}{2\pi} \log S_{\text{BH}}, \quad (38)$$

while the Lyapunov exponent is proportional to the Hawking's temperature.

$$\lambda_L = \frac{2\pi}{\beta}. \quad (39)$$

The butterfly velocity is determined from the near-horizon geometry<sup>5</sup>

$$v_B^2 = \frac{G'_{tt}(r_H)}{(d-1)G'_{ii}(r_H)}. \quad (40)$$

---

<sup>5</sup>Here we are assuming isotropy. In the case of anisotropic metrics the formula for  $v_B$  is a little bit more complicated. See, for instance the appendix A of [41].

## 4.2 Bulk picture for the behaviour of OTOCs

In this section we present the bulk perspective for the vanishing of OTOCs at later times. In order to do that, we write the OTOC as a superposition of two states

$$\text{OTOC}(t) = \langle \text{TFD} | W(-t) V(0) W(-t) V(0) | \text{TFD} \rangle = \langle \psi_{\text{out}} | \psi_{\text{in}} \rangle, \quad (41)$$

where the ‘in’ and ‘out’ states are given by

$$|\psi_{\text{in}}\rangle = W(-t) V(0) | \text{TFD} \rangle, \quad |\psi_{\text{out}}\rangle = V^\dagger(0) W^\dagger(-t) | \text{TFD} \rangle \quad (42)$$

The interpretation of a vanishing OTOC in terms of the bulk theory is actually very simple. Let us go step by step and construct first the state  $V(0)|\beta\rangle$ . This state is described by a particle that comes out of the past horizon, reaches the boundary at  $t = 0$ , and then falls back into the future horizon. See the left panel of figure 10.

Now the ‘in’ state can be obtained as

$$|\psi_{\text{in}}\rangle = W(-t) V(0) | \text{TFD} \rangle = e^{-iHt} W(0) e^{iHt} V(0) | \text{TFD} \rangle. \quad (43)$$

This amounts to evolve the state  $V(0)|\text{TFD}\rangle$  backwards in time, apply the operator  $W$ , and then evolve the system forwards in time. The corresponding description in the bulk is shown in the right panel of figure 10. From this picture we can see that the perturbation  $W$  produces a shock wave that causes a shift in the trajectory of the V-particle, which no longer reaches the boundary at time  $t = 0$ , but rather with some time delay. The physical interpretation is that a small perturbation in the asymptotic past (represented by  $W$ ) is amplified over time and destroys the initial configuration (represented by the state  $V(0)|\text{TFD}\rangle$ ).

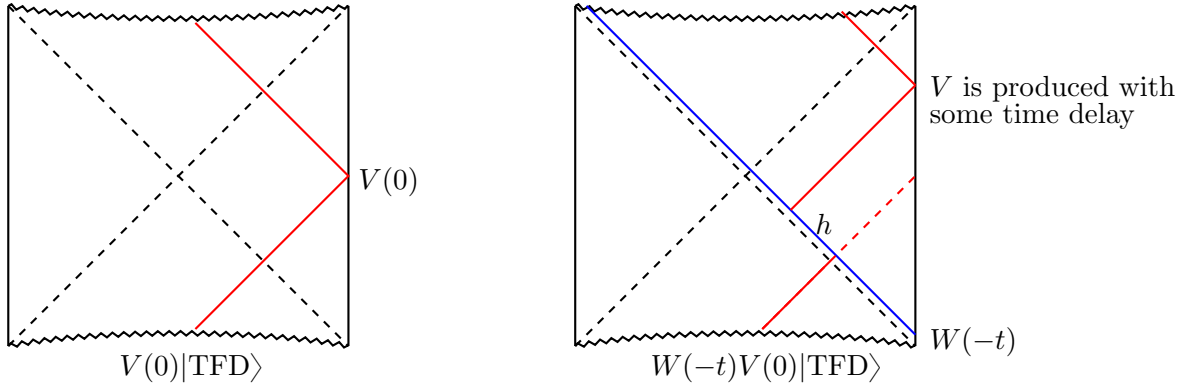


Figure 10: *Left panel*: bulk description of the state  $V(0)|\text{TFD}\rangle$ . The V-particle comes out of the past horizon, reaches the boundary at time  $t = 0$  producing the perturbation  $V$ , and then falls into the future horizon. *Right panel*: bulk description of the ‘in’ state  $|\psi_{\text{in}}\rangle = W(-t)V(0)|\text{TFD}\rangle$ . The W-particle (shown in blue) produces a shock wave along  $V = 0$ . The trajectory of the V-particle (shown in red) suffers a shift and the perturbation  $V$  is produced at the boundary with some time delay.

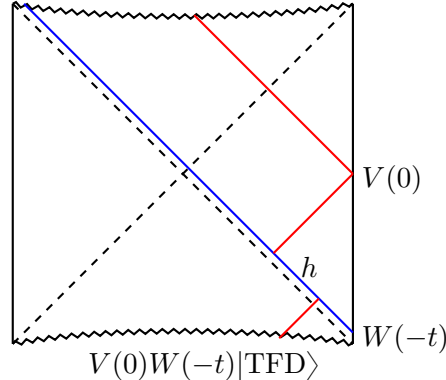


Figure 11: Bulk description of the ‘out’ state  $|\psi_{\text{out}}\rangle = V(0)W(-t)|\text{TFD}\rangle$ . The W-particle produces the shock wave geometry. The trajectory of the V-particle is such that, after suffering the shift  $U \rightarrow U + h(t, \vec{x})$ , reaches the boundary at time  $t = 0$ , producing the perturbation  $V$ .

The bulk description of the ‘out’ state can be obtained in the same way. As this state displays the perturbation  $V$  at  $t = 0$ , the V-particle should be produced in the asymptotic past in such a way that, after its trajectory gets shifted as  $U \rightarrow U + h$ , it reaches the boundary at the time  $t = 0$  producing the perturbation  $V$ .

Comparing the bulk description of the state  $|\psi_{\text{in}}\rangle$  (shown in the right panel of figure 10) with the description of the state  $|\psi_{\text{out}}\rangle$  (shown in figure 11) we can see that

these states are indistinguishable when  $h(t, \vec{x})$  is zero, but they become more and more different for large values of  $h(t, \vec{x})$ . As a consequence, the overlap  $C(t) = \langle \psi_{\text{out}} | \psi_{\text{in}} \rangle$  is equal to one when  $h = 0$ , but it decreases to zero as we increase the value of  $h$ .

The exponential behaviour of  $h(t, \vec{x})$  implies that an early enough perturbation can produce a very large shift in the V-particle's trajectory, causing it to be captured by the black hole, and preventing the materialization of the  $V$  perturbation at the boundary. See figure 12. This should be compared with the physical picture given in figure 3.

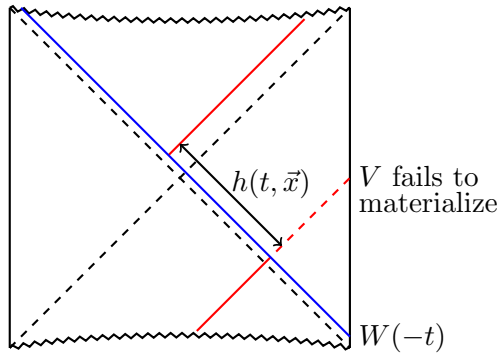


Figure 12: Bulk description of the state  $W(-t)V(0)|\text{TFD}\rangle$  for the case where  $|t| \gtrsim t_*$ . The V-particle's trajectory undergoes a shift, and it is captured by the black hole. The perturbation  $V$  never forms, and the corresponding state have no superposition with the ‘out’ state  $V(0)W(-t)|\text{TFD}\rangle$ , resulting in a vanishing OTOC.

The physical picture of the process described in figure 12 is quite simple. The state  $V(0)|\text{TFD}\rangle$  can be represented by a black hole geometry in which a particle (the V-particle) escapes from the black hole and reaches the boundary at time  $t = 0$ . The state  $W(-t)V(0)|\text{TFD}\rangle$  is obtained by perturbing the state  $V(0)|\text{TFD}\rangle$  in the asymptotic past. This corresponds to add a W-particle to the system in the asymptotic past. This particle gets highly blue shifted as it falls towards the black hole. The black hole captures the W-particle and becomes bigger. The V-particle fails to escape from the bigger black hole, and never reaches the boundary to produce the  $V$  perturbation. This physical picture is illustrated in figure 13.

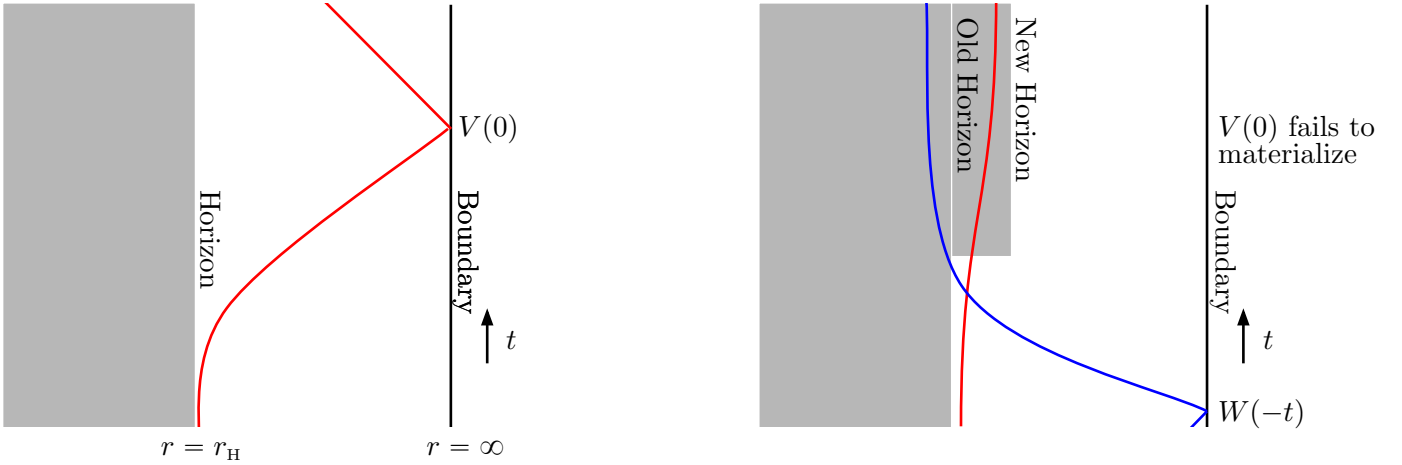


Figure 13: *Left panel*: bulk description of the state  $V(0)|\text{TFD}\rangle$ . The V-particle (whose trajectory is shown in red) escapes from the black hole (shown in gray), reaches the boundary at time  $t = 0$ , and then falls back towards the horizon. *Right panel*: bulk description of the state  $W(-t)V(0)|\text{TFD}\rangle$  for the case where  $|t| \gtrsim t_*$ . The W-particle (whose trajectory is shown in blue) gets blue shifted and increases the black hole size as it falls into it. The V-particle fails to escape from the larger black hole, and the perturbation  $V$  never forms at the boundary.

The precise form of the above OTOC can be obtained by calculating the overlap  $\langle \psi_{\text{out}} | \psi_{\text{in}} \rangle$  using the Eikonal approximation [8], in which the Eikonal phase  $\delta$  is proportional to the shock wave profile  $\delta \sim h(t, \vec{x})$ . The OTOC can be written as an integral of the phase  $e^{i\delta}$  weighted by kinematical factors which are basically Fourier transforms of bulk-to-boundary propagators for the  $V$  and  $W$  operators.

The result for a BTZ black hole reads<sup>6</sup>

$$\frac{\langle V(i\epsilon_1)W(t+i\epsilon_2)V(i\epsilon_3)W(t+i\epsilon_4) \rangle}{\langle V(i\epsilon_1)V(i\epsilon_3) \rangle \langle W(i\epsilon_2)W(i\epsilon_4) \rangle} = \left( \frac{1}{1 - \frac{8\pi i G_N \Delta_W}{\epsilon_{13} \epsilon_{24}^*} e^{\frac{2\pi}{\beta} \left( t - \frac{|\vec{x}|}{v_B} \right)}} \right)^{\Delta_V} \quad (44)$$

where  $\Delta_V$  and  $\Delta_W$  are the scaling dimensions of the operator  $V$  and  $W$ , respectively, and  $\epsilon_{ij} = i(e^{i\epsilon_i} - e^{i\epsilon_j})$ . For this system  $\beta = 2\pi$  and  $v_B = 1$ . This formula matches the direct CFT calculation<sup>7</sup> obtained in [20]. It can also be derived using the geodesic approximation for two-sided correlators in a shock wave background [5, 20].

<sup>6</sup>The above result assumes  $\Delta_W \gg \Delta_V$ .

<sup>7</sup>The CFT perspective for the onset of chaos has been widely discussed in [43]. Other references in this direction include, for instance [44–47].

Expanding the above result for small values of  $G_N e^{\frac{2\pi}{\beta}(t - \frac{|\vec{x}|}{v_B})}$  we obtain

$$\text{OTO}(t) = 1 - 8\pi i G_N \frac{\Delta_V \Delta_W}{\epsilon_{13} \epsilon_{24}^*} e^{\frac{2\pi}{\beta}(t - \frac{|\vec{x}|}{v_B})}, \quad (45)$$

Since  $h(t, \vec{x}) \sim G_N e^{\frac{2\pi}{\beta}(t - \frac{|\vec{x}|}{v_B})}$ , the above result implies

$$C(t, \vec{x}) \sim h(t, \vec{x}). \quad (46)$$

The above result is valid for small<sup>8</sup> values of  $G_N$ , or for any value of  $G_N$ , but for times in the range  $t_d \ll t \ll t_*$ , where  $t_* = \frac{\beta}{2\pi} \log \frac{1}{G_N}$ .

Despite being true for the case of the BTZ black hole, the proportionality between the double commutator and the shock wave profile has not been demonstrated in more general cases. However, the authors of [8] argued that, in regions of moderate scattering between the V- and W-particle, the identification  $C(t, \vec{x}) \sim h(t, \vec{x})$  is approximately valid.

At very late times, the behaviour of the  $\text{OTO}(t)$  is expected to be controlled by the black hole quasi-normal modes. Indeed, in the case of a compact space it is possible to show that

$$C(t) \sim e^{-2i\omega(t-t_*-R/v_B)}, \text{ with } \text{Im}(\omega) < 0, \quad (47)$$

where  $R$  is the diameter of the compact space and  $\omega$  is the system lowest quasi-normal frequency [8].

#### 4.2.1 Stringy corrections

In this section we briefly discuss the effects of stringy corrections to the Einstein gravity results for OTOCs. We start by reviewing the Einstein gravity results from the perspective of scattering amplitudes. In the framework of the Eikonal approximation, the phase shifted suffered by the V-particle is given by

$$\delta = -P^V h(t, \vec{x}) \sim G_N s, \quad (48)$$

where we used the fact that  $h(t, \vec{x}) \sim G_N P^U$  and introduced a Mandelstam-like variable  $s = 2A(0)P^U P^V$ . In a small- $G_N$  expansion the double commutator  $C(t)$  and the phase shift  $\delta$  scale with  $s$  in the same way, namely

$$C(t) \sim G_N s, \quad (49)$$

---

<sup>8</sup>In AdS/CFT the Newton constant is related to the rank of the gauge group of dual CFT as  $G_N \sim 1/N^a$ , where  $a$  is a positive number that depends on the dimensionality of the bulk space time (cf. section 7.2 of [48]). Our classical gravity calculations are only valid in the large- $N$  limit (that suppresses quantum corrections) so it is natural to consider  $G_N$  as a small parameter.

where  $s \sim \beta^{-2} e^{\frac{2\pi}{\beta} t}$ .

The string corrections can be incorporated using the standard Veneziano formula for the relativistic scattering amplitude  $\mathcal{A} \sim s \delta$ . The phase shift can then be schematically written as an infinite sum

$$\delta \sim \sum_J G_N s^{J-1}, \quad (50)$$

where each term correspond to the contribution due to the exchange of a spin  $J$  field. In Einstein gravity the dominant contribution comes from the exchange of a spin-2 field, the graviton. In string theory, we have to include an infinite tower of higher spin fields. Naively, it looks like this higher spin contribution will increase the development of chaos. However, the re-summation of the above sum actually leads to a decrease in the development of chaos. The string-corrected phase shift has a milder dependence with  $s$ , namely

$$\delta \sim G_N s^{J_{\text{eff}}-1}, \quad (51)$$

with the effective spin given by [8]

$$J_{\text{eff}} = 2 - \frac{d(d-1)\ell_s^2}{4\ell_{AdS}^2} \quad (52)$$

where  $\ell_s$  is the string length,  $\ell_{AdS}$  is the AdS length scale and  $d$  is the number of dimensions of the boundary theory. As a result, the string-corrected double commutator grows in time with an effective smaller Lyapunov exponent

$$C_{\text{string}}(t) \sim e^{\frac{2\pi}{\beta} \left(1 - \frac{d(d-1)\ell_s^2}{4\ell_{AdS}^2}\right) t}, \quad (53)$$

and this leads to a larger scrambling time<sup>9</sup>

$$t_*^{\text{string}} = t_* \left(1 + \frac{d(d-1)\ell_s^2}{4\ell_{AdS}^2}\right). \quad (54)$$

The above discussion implies that for a theory with a finite number of high-spin fields ( $J > 2$ ) chaos would develop faster than in Einstein gravity. These theories, however, are known to violate causality [50]. It is then natural to speculate that the Lyapunov exponent obtained in Einstein gravity has the maximal possible value allowed by causality. This is indeed true and this is the topic of the next section.

---

<sup>9</sup>At small scales, the string-corrected shock wave has a gaussian profile, and the concept of butterfly velocity is not meaningful. It was recently shown, however, that at larger scales is possible to define a string-corrected butterfly velocity. The result for  $\mathcal{N} = 4$  SYM theory reads [49]  $v_B = \sqrt{\frac{2}{3}} \left(1 + \frac{23\zeta(3)}{16} \frac{1}{\lambda^{3/2}}\right)$ , where  $\lambda$  is the 't Hooft coupling, which can be written in terms of string length scale as  $\lambda = (\ell_{AdS}/\ell_s)^4$ .

### 4.2.2 Bounds on chaos

In holographic theories, the dissipation time is controlled by the black hole quasinormal modes, so one generally expects  $t_d \sim \beta$  for low dimension operators. On the other hand, the scrambling time for black holes is found to be  $t_* \sim \beta \log N^2$ . For general quantum systems with such a large hierarchy between these two time scales,  $t_d \ll t_*$ , the Lyapunov exponent was shown to have a sharp upper bound [42]

$$\lambda_L \leq \frac{2\pi}{\beta}. \quad (55)$$

Interestingly, this bound is saturated by black holes in Einstein gravity, leading to the speculation that any large  $N$  system that saturates this bound will necessarily have an Einstein gravity dual, at least in the near horizon region [42, 9]. Such a claim triggered an enormous interest in the community, and lead to many works attempting to use the saturation of the bound as a criterion to discriminate between CFTs with potential Einstein gravity duals [20, 43–47, 51, 52]. However, it was recently proved that this criterion by itself is insufficient (albeit necessary) to guarantee a dual description with gravitational degrees of freedom [53, 54].

Since  $v_B$  defines the speed at which information propagates it is natural to question whether this quantity is also bounded. In [55] it was proved that for asymptotically AdS black holes in two-derivative (Einstein) gravity, satisfying null energy condition (NEC), the butterfly velocity is bounded by

$$v_B \leq v_B^{\text{Sch}} = \sqrt{\frac{d}{2(d-1)}}, \quad (56)$$

where  $v_B^{\text{Sch}}$  is the value of the butterfly velocity for a  $(d+1)$ -dimensional AdS-Schwarzschild black brane. It is tempting to conjecture that (56) might be a bound for any (local) QFT, in the same sense as the bound for the Lyapunov exponent (55). However, (56) was shown to fail for higher derivative gravities [7], as well as for anisotropic theories in Einstein gravity [56, 57], which is reminiscent of the well-known violation of the shear viscosity to entropy density ratio [58–63]. In such cases, however,  $v_B$  is still bounded from above and never reaches the speed of light  $c = 1$ , provided that the theory respects causality.<sup>10</sup> Naively, one would expect the speed of light to define a region of causal influence in a relativistic system. However, as clarified in [64], when we only have access to a subset of the Hilbert space, the propagation velocity of causal influence is generically smaller than the speed of light. So, we usually have  $v_B < 1$

---

<sup>10</sup>The butterfly velocity can exceed the speed of light if causality is violated. For instance, Gauss-Bonnet gravity in  $d = 4$  dimensions has  $v_B > 1$  for  $\lambda_{\text{GB}} < -0.75$ . However, causality only holds for  $\lambda_{\text{GB}} > -0.19$  [65, 66] (furthermore, it requires an infinite tower of extra higher spin fields [50]).

because the butterfly velocity characterizes the velocity of causal influence in a subset of the Hilbert space defined by the thermal ensemble, i.e. the states with a fixed energy density. Indeed, the authors of [64] showed that, for any asymptotically AdS geometry in two-derivative gravity, the butterfly velocity is bounded by the speed of light, i.e.

$$v_B \leq 1, \quad (57)$$

as it should for a theory with a (Lorentz invariant) UV fixed point. In the case of non-Lorentz invariant theories, like, for instance, non-commutative gauge theories, non-local effects lead to the violation of such bound [41].

Lastly, we discuss a lower bound for the scrambling time. In black hole physics the scrambling time defines how fast the information that has fallen into a black hole can be recovered from the emitted Hawking radiation<sup>11</sup>. In the context of the Hayden-Preskill thought experiment, the scrambling time is barely compatible with black hole complementarity [67], since a smaller scrambling time would lead to a violation of the non-cloning principle. This led Susskind and Sekino to conjecture that black holes were the fastest scramblers in nature, i.e., they have the smallest possible scrambling time [68].

### 4.3 Chaos and Spreading of Entanglement

The thermofield double state displays a very atypical left-right pattern of entanglement that results from non-zero correlations between subsystems of  $\text{QFT}_L$  and  $\text{QFT}_R$  at  $t = 0$ . The chaotic nature of the boundary theories is manifest by the fact that small perturbations added to the system in the asymptotic past destroy this delicate correlations [5].

The special pattern of entanglement can be efficiently diagnosed by considering the mutual information  $I(A, B)$  between spatial subsystems  $A \subset \text{QFT}_L$  and  $B \subset \text{QFT}_R$ , defined as

$$I(A, B) = S_A + S_B - S_{A \cup B}, \quad (58)$$

where  $S_A$  is the entanglement entropy of the subsystem  $A$ , and so on. The mutual information is always positive and provides an upper bound for correlations between operators  $\mathcal{O}_L$  and  $\mathcal{O}_R$  defined on  $A$  and  $B$ , respectively [69]

$$I(A, B) \geq \frac{(\langle \mathcal{O}_L \mathcal{O}_R \rangle - \langle \mathcal{O}_L \rangle \langle \mathcal{O}_R \rangle)^2}{2\langle \mathcal{O}_L^2 \rangle \langle \mathcal{O}_R^2 \rangle}. \quad (59)$$

---

<sup>11</sup>This assumes that half of the black hole's initial entropy has been radiated.

The thermofield double state has non-zero mutual information between large<sup>12</sup> subsystems of the left and right boundary, signaling the existence of left-right correlations. These correlations can be destroyed by small perturbations in the asymptotic past, meaning that an initially positive mutual information drops to zero when we add a very early perturbation to the system.

Interestingly, the vanishing of the mutual information can be connected to the vanishing of the OTOCs discussed earlier. If, for simplicity, we assume that  $\mathcal{O}_L$  and  $\mathcal{O}_R$  have zero thermal one point function, then the disruption of the mutual information implies the vanishing of the following four point function

$$\langle \mathcal{O}_L \mathcal{O}_R \rangle_W = \langle \text{TFD} | W_R^\dagger \mathcal{O}_L \mathcal{O}_R W_R | \text{TFD} \rangle = 0, \quad (60)$$

which is related by analytic continuation to the one-sided out-of-time-order correlator introduced earlier<sup>13</sup>.

The disruption of the mutual information has a very simple geometrical realization in the bulk. The entanglement entropies that appear in the definition of  $I(A, B)$  can be holographically calculated using the HRRT prescription [70, 71]

$$S_A = \frac{\text{Area}(\gamma_A)}{4G_N}, \quad (61)$$

where  $\gamma_A$  is an extremal surface whose boundary coincides with the boundary of the region  $A$ . There is an analogous formula for  $S_B$ . Both  $\gamma_A$  and  $\gamma_B$  are U-shaped surfaces lying outside of the event horizon, in the left and right side of the geometry, respectively. The last term,  $S_{A \cup B}$ , is given by the area of the extremal surface whose boundary coincides with the boundary of  $A \cup B$ . There are two candidates for this extremal surfaces. The first one is the surface  $\gamma_A \cup \gamma_B$ , while the second one is the surface  $\gamma_{\text{wormhole}}$  that stretches through the wormhole connecting the two boundaries of the geometry. See figure 1 (a) for a schematic illustration. If the surface  $\gamma_A \cup \gamma_B$  has less area than the surface  $\gamma_{\text{wormhole}}$ , then we have  $I(A, B) = 0$ , because  $\text{Area}(\gamma_A \cup \gamma_B) = \text{Area}(\gamma_A) + \text{Area}(\gamma_B)$ . On the other hand, if  $\gamma_{\text{wormhole}}$  has less area than  $\gamma_A \cup \gamma_B$ , then we have that  $\text{Area}(\gamma_A \cup \gamma_B) < \text{Area}(\gamma_A) + \text{Area}(\gamma_B)$ , resulting in a positive mutual information  $I(A, B) > 0$ .

With the above formulas a non-zero mutual information can be written as

$$I(A, B) = \frac{1}{4G_N} [\text{Area}(\gamma_A) + \text{Area}(\gamma_B) - \text{Area}(\gamma_{\text{wormhole}})]. \quad (62)$$

Now, an early perturbation of the thermofield double state gives rise to a shock wave geometry in which the wormhole becomes longer. As a consequence the area of the

---

<sup>12</sup>For small subsystems, the mutual information is zero.

<sup>13</sup>To obtain an OTOC with operators acting only on the right boundary theory one just need to add  $i\beta/2$  to time argument of the operator  $\mathcal{O}_L$  in the above formula.

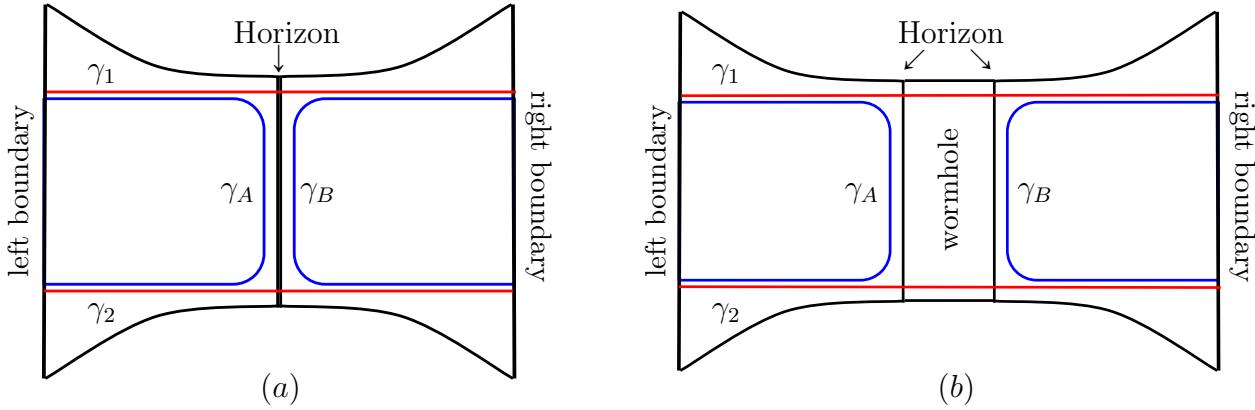


Figure 14: Schematic representation of the  $t = 0$  slice of (a) the unperturbed two-sided black brane geometry and (b) the two-sided black brane geometry in the presence of a shock wave. We assume that the shock wave is sent at some time  $-t < 0$ , therefore, it effectively increases the size of the wormhole at  $t = 0$ . In both cases the blue curves represent the U-shaped extremal surfaces  $\gamma_A$  (in the left side of the geometry) and  $\gamma_B$  (in the right side of the geometry). The red curves represent extremal surfaces  $\gamma_1$  and  $\gamma_2$  connecting the two sides of the geometry. The extremal surface  $\gamma_{\text{wormhole}}$  defined in the text is given by the union of these two surfaces,  $\gamma_{\text{wormhole}} = \gamma_1 \cup \gamma_2$ .

surface  $\gamma_{\text{wormhole}}$  increases, resulting in a smaller mutual information. See figure 1 for an illustration. It is then clear that the mutual information will drop to zero if the wormhole is longer enough. The length of the wormhole depends on the strength of the shock wave, which, by its turn, depends on how early is the perturbation producing it. Therefore, an early enough perturbation will produce a very long wormhole in which the mutual information will be zero. The fact that the shock wave geometry produces a longer wormhole (along the  $t = 0$  slice of the geometry) is clearly seen if we represent the shock wave geometry with a tilted Penrose diagram. See, for instance, the figure 3 of [72].

The mutual information  $I(A, B)$  decreases as a function of the time  $t_0$  at which we perturbed the system. For  $t_0 \gtrsim t_*$ , the mutual information decreases linearly with behaviour controlled by the so-called entanglement velocity  $v_E$  [57]

$$\frac{dI(A, B)}{dt_0} = -\frac{dS_{A \cup B}}{dt_0} = -v_E s_{\text{th}} A_\Sigma, \quad (63)$$

where  $s_{\text{th}}$  is the thermal entropy density and  $A_\Sigma$  is the area of  $\Sigma = \partial(A \cup B)$ . This behavior can be understood in terms of the so-called ‘entanglement tsunami’ picture that appears in the study of entanglement entropy following a quantum quench, both in field

theory [81] and holographic calculations [82–86]. In [85, 86], the authors conjectured the entanglement velocity should be bounded by

$$v_E \leq v_E^{\text{Sch}} = \frac{\sqrt{d}(d-1)^{\frac{1}{2}-\frac{1}{d}}}{[2(d-1)]^{1-\frac{1}{d}}}, \quad (64)$$

where  $v_E^{\text{Sch}}$  is the entanglement velocity for a  $(d+1)$ -dimensional Schwarzschild black brane. Later in [55], this bound was proven to be valid for quite generic holographic theories in Einstein gravity satisfying the NEC. However, this bound was shown to be violated once the assumption of isotropy is relaxed [57, 80]. In this case, though,  $v_E$  is still bounded and never exceeds the speed of light.

More generally, [87] conjectured that in any quantum system  $v_E \leq v_B$ . So, if the bound  $v_B \leq 1$  holds true, then, the entanglement velocity must also be bounded

$$v_E \leq 1. \quad (65)$$

The authors of [88] proved this using the positivity of mutual information, while [89] used inequalities of relative entropy.<sup>14</sup> However, both [88, 89] assumed that the theory is Lorentz invariant. In the case of non-Lorentz invariant theories, like non-commutative gauge theories, for example, the entanglement velocity can surpass the speed of light. This has been verified both in holography calculations [41] and in field theory calculations [90].

Finally, we mention that other concepts from information theory can also be used to diagnose chaos. It has been shown, for instance, that the relative entropy is also a useful tool to diagnose chaotic behaviour [93]. For a connection between chaos and computational complexity, see, for instance [94, 95].

## 4.4 Chaos & Hydrodynamics

Recently, there has been a growing interest in the connection between chaos and hydrodynamics [96–104]. Here we briefly review some interesting connection between chaos and diffusion phenomena.

The Lyapunov exponent defines a time scale known as *Lyapunov time*, which is given by  $t_L = 1/\lambda_L$ . The upper bound in  $\lambda_L$  implies a lower bound in the Lyapunov time  $t_L \geq \frac{\beta}{2\pi}$ .<sup>15</sup> For convenience, let us call  $\tau_L$  the lower bound on the Lyapunov time.

---

<sup>14</sup>Strictly speaking, the bound (65) holds true for large enough subsystems. For small subsystems, the ‘entanglement tsunami’ picture breaks down and (65) can be violated instantaneously [91, 92]. However, causality still implies that in average,  $v_E^{\text{avg}} < 1$  throughout a unitary evolution.

<sup>15</sup>Here we are using units such that Planck and Boltzmann constants  $\hbar$  and  $k_B$  are both equal to unity. If we reintroduce  $\hbar$  and  $k_B$  in our formulas we obtain  $\lambda_L \leq \frac{2\pi k_B}{\hbar\beta}$  or  $t_L \geq \frac{\hbar\beta}{2\pi k_B}$ .

In [105, 106] it was proposed that  $\tau_L = \hbar/(2\pi k_B T)$  provides a fundamental dissipative time scale that controls the transport in strongly coupled systems. Such a universal time scale would be responsible for the universal properties of several strongly coupled systems that do not have a description in terms of quasiparticle excitations. Working on these ideas and aiming to explain the linear- $T$  resistivity behavior of strange metals, Hartnoll [107] proposed the existence of a universal bound on the diffusion constants related to the collective diffusion of charge and energy  $D \gtrsim \hbar v^2/(k_B T)$ , where  $v$  is some characteristic velocity of the theory. As the thermoelectric diffusion constant  $D$  is proportional to the conductivity  $\sigma$ , the saturation of the lower bound on  $D$  implies the scaling  $\sigma \sim 1/T$ , that results in a linear- $T$  resistivity behavior.

In an holographic treatment, both the transport and the chaotic properties of the gauge theory are determined by the dynamics close to the black hole horizon in the gravitational dual. It is then natural to question if there is any connection between chaos and diffusion phenomena. With this in mind, Blake proposed in [96, 97] that, for particle-hole symmetric theories, the electric diffusivity  $D_c$  should be controlled by  $v_B$  and  $\tau_L$  as

$$D_c \geq C_c v_B^2 \tau_L, \quad (66)$$

where  $C_c$  is a constant that depended on the universality class of theory. The above proposal works well for system where energy and charge diffuse independently, but it is not valid in more general situations. See, for instance [108–112].

In [113] it was proposed that, for a general family of holographic Q-lattice models, the thermal diffusivity  $D_T$  should be generically related to chaos exponents at infrared fixed points through

$$D_T \geq C_T v_B^2 \tau_L, \quad (67)$$

where  $C_T$  is another universality constant different from  $C_c$  (this was latter generalized to theories with an spatial anisotropy in [114]). This Q-lattice models do not have translational symmetry and features a finite charge density, which makes  $D_T$  finite.

## 5 Closing remarks

The holographic description of quantum chaos not only has provide new insights into the inner-workings of gauge-gravity duality, but it has also provided insights outside the scope of holography: some examples include the characterization of chaos with OTOCs, the definition of a quantum Lyapunov exponent and the existence of a bound for chaos.

The success of this new approach to quantum chaos explains the growing experimental interest that OTOCs have been received. Indeed, several protocols for measuring

OTOCs have been proposed, and there is already a few experimental results. See [115] and references therein.

Finally, one of the remarkable features of quantum chaos is level statistics described by random matrices. The fact that this is present in the infrared limit of the SYK model [116–118] suggests that it also should be present in quantum black holes<sup>16</sup>, although this has not yet been verified [119].

## Acknowledgments

It is a pleasure to thank A. M. García-García, S. Nicolis, and S. A. H. Mansoori for useful correspondence.

## Conflicts of Interest

The author declares that there is no conflict of interest regarding the publication of this paper.

## References

- [1] D. Ullmo, S. Tomsovic, “Introduction to quantum chaos”, <http://www.lptms.u-psud.fr/membres/ullmo/Articles/eolss-ullmo-tomsovic.pdf>, (2014)
- [2] J. M. Maldacena, “The large  $N$  limit of superconformal field theories and supergravity,” *Adv. Theor. Math. Phys.* **2**, 231 (1998) [*Int. J. Theor. Phys.* **38**, 1113 (1999)] [[hep-th/9711200](#)].
- [3] S. S. Gubser, I. R. Klebanov, A. M. Polyakov, “Gauge theory correlators from noncritical string theory,” *Phys. Lett.* **B428**, 105-114 (1998) [[hep-th/9802109](#)].
- [4] E. Witten, “Anti-de Sitter space and holography,” *Adv. Theor. Math. Phys.* **2**, 253-291 (1998) [[hep-th/9802150](#)].
- [5] S. H. Shenker and D. Stanford, “Black holes and the butterfly effect,” *JHEP* **1403**, 067 (2014) [[arXiv:1306.0622 \[hep-th\]](#)].
- [6] S. H. Shenker and D. Stanford, “Multiple Shocks,” *JHEP* **1412**, 046 (2014) [[arXiv:1312.3296 \[hep-th\]](#)].

---

<sup>16</sup>We thank A. M. García-García for calling our attention to this.

- [7] D. A. Roberts, D. Stanford and L. Susskind, “Localized shocks,” *JHEP* **1503**, 051 (2015) [arXiv:1409.8180 [hep-th]].
- [8] S. H. Shenker and D. Stanford, “Stringy effects in scrambling,” *JHEP* **1505**, 132 (2015) [arXiv:1412.6087 [hep-th]].
- [9] A. Kitaev, “Hidden Correlations in the Hawking Radiation and Thermal Noise,” talk given at Fundamental Physics Prize Symposium, Nov. 10, 2014. Stanford SITP seminars, Nov. 11 and Dec. 18, 2014.
- [10] E. B. Rozenbaum, S. Ganeshan and V. Galitski, “Lyapunov Exponent and Out-of-Time-Ordered Correlator’s Growth Rate in a Chaotic System”, *Phys. Rev. Lett.* **188**, 086801, 2017.
- [11] E. B. Rozenbaum, S. Ganeshan and V. Galitski, “Universal Level Statistics of the Out-of-Time-Ordered Operator”, arXiv:1801.10591 [cond-mat.dis-nn].
- [12] J. Chávez-Carlos, B. López-Del-Carpio, M. A. Bastarrachea-Magnani, P. Stránský, S. Lerma-Hernández, L. F. Santos and J. G. Hirsch, “Quantum and Classical Lyapunov Exponents in Atom-Field Interaction Systems,” arXiv:1807.10292 [cond-mat.stat-mech].
- [13] J. Polchinski and V. Rosenhaus, “The Spectrum in the Sachdev-Ye-Kitaev Model,” *JHEP* **1604**, 001 (2016) doi:10.1007/JHEP04(2016)001 [arXiv:1601.06768 [hep-th]].
- [14] J. Maldacena and D. Stanford, “Remarks on the Sachdev-Ye-Kitaev model,” *Phys. Rev. D* **94**, no. 10, 106002 (2016) doi:10.1103/PhysRevD.94.106002 [arXiv:1604.07818 [hep-th]].
- [15] J. Maldacena, D. Stanford and Z. Yang, “Conformal symmetry and its breaking in two dimensional Nearly Anti-de-Sitter space,” *PTEP* **2016**, no. 12, 12C104 (2016) doi:10.1093/ptep/ptw124 [arXiv:1606.01857 [hep-th]].
- [16] A. Kitaev and S. J. Suh, “The soft mode in the Sachdev-Ye-Kitaev model and its gravity dual,” *JHEP* **1805**, 183 (2018) doi:10.1007/JHEP05(2018)183 [arXiv:1711.08467 [hep-th]].
- [17] M. Axenides, E. G. Floratos and S. Nicolis, “Modular discretization of the  $AdS_2/CFT_1$  holography,” *JHEP* **1402**, 109 (2014) doi:10.1007/JHEP02(2014)109 [arXiv:1306.5670 [hep-th]].
- [18] M. Axenides, E. Floratos and S. Nicolis, “Chaotic Information Processing by Extremal Black Holes,” *Int. J. Mod. Phys. D* **24**, no. 09, 1542012 (2015) doi:10.1142/S0218271815420122 [arXiv:1504.00483 [hep-th]].
- [19] M. Axenides, E. Floratos and S. Nicolis, “The quantum cat map on the modular discretization of extremal black hole horizons,” *Eur. Phys. J. C* **78**, no. 5, 412 (2018) doi:10.1140/epjc/s10052-018-5850-9 [arXiv:1608.07845 [hep-th]].

- [20] D. A. Roberts and D. Stanford, “Two-dimensional conformal field theory and the butterfly effect,” *Phys. Rev. Lett.* **115**, no. 13, 131603 (2015) [arXiv:1412.5123 [hep-th]].
- [21] D. Stanford, “Many-body chaos at weak coupling,” *JHEP* **1610**, 009 (2016) doi:10.1007/JHEP10(2016)009 [arXiv:1512.07687 [hep-th]].
- [22] E. Plamadeala and E. Fradkin, “Scrambling in the quantum Lifshitz model,” *J. Stat. Mech.* **1806**, no. 6, 063102 (2018). doi:10.1088/1742-5468/aac136
- [23] A. Nahum, S. Vijay and J. Haah, “Operator Spreading in Random Unitary Circuits,” *Phys. Rev. X* **8**, no. 2, 021014 (2018) doi:10.1103/PhysRevX.8.021014 [arXiv:1705.08975 [cond-mat.str-el]].
- [24] V. Khemani, A. Vishwanath and D. A. Huse, “Operator spreading and the emergence of dissipation in unitary dynamics with conservation laws,” *Phys. Rev. X* **8**, no. 3, 031057 (2018) doi:10.1103/PhysRevX.8.031057 [arXiv:1710.09835 [cond-mat.stat-mech]].
- [25] T. Rakovszky, F. Pollmann and C. W. von Keyserlingk, “Diffusive hydrodynamics of out-of-time-ordered correlators with charge conservation,” *Phys. Rev. X* **8**, no. 3, 031058 (2018) doi:10.1103/PhysRevX.8.031058 [arXiv:1710.09827 [cond-mat.stat-mech]].
- [26] D. J. Luitz and Y. Bar Lev, “Information propagation in isolated quantum systems,” *Phys. Rev. B* **96**, no. 2, 020406 (2017) doi:10.1103/PhysRevB.96.020406 [arXiv:1702.03929 [cond-mat.dis-nn]].
- [27] A. Bohrdt, C. B. Mendl, M. Endres and M. Knap, “Scrambling and thermalization in a diffusive quantum many-body system,” *New J. Phys.* **19**, no. 6, 063001 (2017) doi:10.1088/1367-2630/aa719b [arXiv:1612.02434 [cond-mat.quant-gas]].
- [28] M. Heyl, F. Pollman, and B. Dóra, “Detecting Equilibrium and Dynamical Quantum Phase Transitions in Ising Chains via Out-of-Time-Ordered Correlators,” *Phys. Rev. Lett.* **121**, 016801 (2018) doi:10.1103/PhysRevLett.121.016801
- [29] C-J. Lin, O. I. Motrunich, “Out-of-time-ordered correlators in quantum Ising chain,” *Phys. Rev. B* **97**, 144304 (2018) doi:10.1103/PhysRevB.97.144304
- [30] S. Xu and B. Swingle, “Accessing scrambling using matrix product operators,” arXiv:1802.00801 [quant-ph].
- [31] M. Cencini, F. Cecconi and A. Vulpiani, “Chaos: From Simple Models to Complex Systems,” World Scientific: Singapore, 2009.
- [32] J. Polchinski, “Chaos in the black hole S-matrix,” arXiv:1505.08108 [hep-th].
- [33] D. Stanford, “Many-body quantum chaos,” Seminar at the school *IAS PiTP 2018: From Qubits to Spacetime*. <https://video.ias.edu/PiTP/2018/0723-DouglasStanford>

- [34] A. I. Larkin and Y. N. Ovchinnikov, “Quasiclassical method in the theory of superconductivity,” JETP 28, 6 (1969), 1200-1205.
- [35] V. Khemani, D. A. Huse and A. Nahum, “Velocity-dependent Lyapunov exponents in many-body quantum, semiclassical, and classical chaos,” Phys. Rev. B **98**, no. 14, 144304 (2018) doi:10.1103/PhysRevB.98.144304 [arXiv:1803.05902 [cond-mat.stat-mech]].
- [36] D. A. Roberts and B. Swingle, “Lieb-Robinson Bound and the Butterfly Effect in Quantum Field Theories,” Phys. Rev. Lett. **117**, no. 9, 091602 (2016) [arXiv:1603.09298 [hep-th]].
- [37] J. M. Maldacena, “Eternal black holes in anti-de Sitter,” JHEP **0304**, 021 (2003) [hep-th/0106112].
- [38] L. Fidkowski, V. Hubeny, M. Kleban and S. Shenker, “The Black hole singularity in AdS / CFT,” JHEP **0402**, 014 (2004) doi:10.1088/1126-6708/2004/02/014 [hep-th/0306170].
- [39] T. Dray and G. ’t Hooft, “The Gravitational Shock Wave of a Massless Particle,” Nucl. Phys. B **253**, 173 (1985).
- [40] K. Sfetsos, “On gravitational shock waves in curved space-times,” Nucl. Phys. B **436**, 721 (1995) [hep-th/9408169].
- [41] W. Fischler, V. Jahnke and J. F. Pedraza, “Chaos and entanglement spreading in a non-commutative gauge theory,” JHEP **1811**, 072 (2018) doi:10.1007/JHEP11(2018)072 [arXiv:1808.10050 [hep-th]].
- [42] J. Maldacena, S. H. Shenker and D. Stanford, “A bound on chaos,” JHEP **1608**, 106 (2016) [arXiv:1503.01409 [hep-th]].
- [43] E. Perlmutter, “Bounding the Space of Holographic CFTs with Chaos,” JHEP **1610**, 069 (2016) [arXiv:1602.08272 [hep-th]].
- [44] A. L. Fitzpatrick and J. Kaplan, “A Quantum Correction To Chaos,” JHEP **1605**, 070 (2016) [arXiv:1601.06164 [hep-th]].
- [45] P. Caputa, T. Numasawa and A. Veliz-Osorio, “Out-of-time-ordered correlators and purity in rational conformal field theories,” PTEP **2016**, no. 11, 113B06 (2016) [arXiv:1602.06542 [hep-th]].
- [46] G. Turiaci and H. Verlinde, “On CFT and Quantum Chaos,” JHEP **1612**, 110 (2016) [arXiv:1603.03020 [hep-th]].
- [47] P. Caputa, Y. Kusuki, T. Takayanagi and K. Watanabe, “Out-of-Time-Ordered Correlators in  $(T^2)^n/\mathbb{Z}_n$ ,” Phys. Rev. D **96**, no. 4, 046020 (2017) [arXiv:1703.09939 [hep-th]].

[48] M. Taylor, “Generalized conformal structure, dilaton gravity and SYK,” *JHEP* **1801**, 010 (2018) doi:10.1007/JHEP01(2018)010 [arXiv:1706.07812 [hep-th]].

[49] S. Grozdanov, “On the connection between hydrodynamics and quantum chaos in holographic theories with stringy corrections,” arXiv:1811.09641 [hep-th].

[50] X. O. Camanho, J. D. Edelstein, J. Maldacena and A. Zhiboedov, “Causality Constraints on Corrections to the Graviton Three-Point Coupling,” *JHEP* **1602**, 020 (2016) [arXiv:1407.5597 [hep-th]].

[51] B. Michel, J. Polchinski, V. Rosenhaus and S. J. Suh, “Four-point function in the IOP matrix model,” *JHEP* **1605**, 048 (2016) [arXiv:1602.06422 [hep-th]].

[52] P. Padmanabhan, S. J. Rey, D. Teixeira and D. Trancanelli, “Supersymmetric many-body systems from partial symmetries integrability, localization and scrambling,” *JHEP* **1705**, 136 (2017) doi:10.1007/JHEP05(2017)136 [arXiv:1702.02091 [hep-th]].

[53] J. de Boer, E. Llabrés, J. F. Pedraza and D. Vegh, “Chaotic strings in AdS/CFT,” *Phys. Rev. Lett.* **120**, no. 20, 201604 (2018) [arXiv:1709.01052 [hep-th]].

[54] A. Banerjee, A. Kundu and R. R. Poojary, “Strings, Branes, Schwarzian Action and Maximal Chaos,” arXiv:1809.02090 [hep-th].

[55] M. Mezei, “On entanglement spreading from holography,” *JHEP* **1705**, 064 (2017) [arXiv:1612.00082 [hep-th]].

[56] D. Giataganas, U. Gürsoy and J. F. Pedraza, “Strongly-coupled anisotropic gauge theories and holography,” arXiv:1708.05691 [hep-th].

[57] V. Jahnke, “Delocalizing entanglement of anisotropic black branes,” *JHEP* **1801**, 102 (2018) [arXiv:1708.07243 [hep-th]].

[58] M. Brigante, H. Liu, R. C. Myers, S. Shenker and S. Yaida, “Viscosity Bound Violation in Higher Derivative Gravity,” *Phys. Rev. D* **77**, 126006 (2008) [arXiv:0712.0805 [hep-th]].

[59] M. Brigante, H. Liu, R. C. Myers, S. Shenker and S. Yaida, “The Viscosity Bound and Causality Violation,” *Phys. Rev. Lett.* **100**, 191601 (2008) [arXiv:0802.3318 [hep-th]].

[60] X. O. Camanho, J. D. Edelstein and M. F. Paulos, “Lovelock theories, holography and the fate of the viscosity bound,” *JHEP* **1105**, 127 (2011) [arXiv:1010.1682 [hep-th]].

[61] J. Erdmenger, P. Kerner and H. Zeller, “Non-universal shear viscosity from Einstein gravity,” *Phys. Lett. B* **699**, 301 (2011) [arXiv:1011.5912 [hep-th]].

[62] A. Rebhan and D. Steineder, “Violation of the Holographic Viscosity Bound in a Strongly Coupled Anisotropic Plasma,” *Phys. Rev. Lett.* **108**, 021601 (2012) [arXiv:1110.6825 [hep-th]].

[63] V. Jahnke, A. S. Misobuchi and D. Trancanelli, “Holographic renormalization and anisotropic black branes in higher curvature gravity,” *JHEP* **1501**, 122 (2015) [arXiv:1411.5964 [hep-th]].

[64] X. L. Qi and Z. Yang, “Butterfly velocity and bulk causal structure,” arXiv:1705.01728 [hep-th].

[65] X. O. Camanho and J. D. Edelstein, “Causality constraints in AdS/CFT from conformal collider physics and Gauss-Bonnet gravity,” *JHEP* **1004**, 007 (2010) [arXiv:0911.3160 [hep-th]].

[66] A. Buchel, J. Escobedo, R. C. Myers, M. F. Paulos, A. Sinha and M. Smolkin, “Holographic GB gravity in arbitrary dimensions,” *JHEP* **1003**, 111 (2010) [arXiv:0911.4257 [hep-th]].

[67] P. Hayden and J. Preskill, “Black holes as mirrors: Quantum information in random subsystems,” *JHEP* **0709**, 120 (2007) [arXiv:0708.4025 [hep-th]].

[68] Y. Sekino and L. Susskind, “Fast Scramblers,” *JHEP* **0810**, 065 (2008) [arXiv:0808.2096 [hep-th]].

[69] M. M. Wolf, F. Verstraete, M. B. Hastings, and J. I. Cirac, “Area laws in quantum systems: Mutual information and correlations”, *Phys. Rev. Lett.* **100**, 070502 (2008) [arXiv:0704.3906 [quant-ph]].

[70] S. Ryu and T. Takayanagi, “Holographic derivation of entanglement entropy from AdS/CFT,” *Phys. Rev. Lett.* **96**, 181602 (2006) [hep-th/0603001].

[71] V. E. Hubeny, M. Rangamani and T. Takayanagi, “A Covariant holographic entanglement entropy proposal,” *JHEP* **0707**, 062 (2007) [arXiv:0705.0016 [hep-th]].

[72] S. Leichenauer, “Disrupting Entanglement of Black Holes,” *Phys. Rev. D* **90**, no. 4, 046009 (2014) [arXiv:1405.7365 [hep-th]].

[73] N. Sircar, J. Sonnenschein and W. Tangarife, “Extending the scope of holographic mutual information and chaotic behavior,” *JHEP* **1605**, 091 (2016) [arXiv:1602.07307 [hep-th]].

[74] Y. Ling, P. Liu and J. P. Wu, “Holographic Butterfly Effect at Quantum Critical Points,” *JHEP* **1710**, 025 (2017) [arXiv:1610.02669 [hep-th]].

[75] R. G. Cai, X. X. Zeng and H. Q. Zhang, “Influence of inhomogeneities on holographic mutual information and butterfly effect,” *JHEP* **1707**, 082 (2017) [arXiv:1704.03989 [hep-th]].

- [76] M. M. Qaemmaqami, “Criticality in third order Lovelock gravity and butterfly effect,” *Eur. Phys. J. C* **78**, no. 1, 47 (2018) [arXiv:1705.05235 [hep-th]].
- [77] S. F. Wu, B. Wang, X. H. Ge and Y. Tian, “Holographic RG flow of thermoelectric transport with momentum dissipation,” *Phys. Rev. D* **97**, no. 6, 066029 (2018) [arXiv:1706.00718 [hep-th]].
- [78] M. M. Qaemmaqami, “Butterfly effect in 3D gravity,” *Phys. Rev. D* **96**, no. 10, 106012 (2017) [arXiv:1707.00509 [hep-th]].
- [79] H. S. Jeong, Y. Ahn, D. Ahn, C. Niu, W. J. Li and K. Y. Kim, “Thermal diffusivity and butterfly velocity in anisotropic Q-Lattice models,” *JHEP* **1801**, 140 (2018) [arXiv:1708.08822 [hep-th]].
- [80] D. Avila, V. Jahnke and L. Patiño, “Chaos, Diffusivity, and Spreading of Entanglement in Magnetic Branes, and the Strengthening of the Internal Interaction,” *JHEP* **1809**, 131 (2018) doi:10.1007/JHEP09(2018)131 [arXiv:1805.05351 [hep-th]].
- [81] P. Calabrese and J. L. Cardy, “Evolution of entanglement entropy in one-dimensional systems,” *J. Stat. Mech.* **0504**, P04010 (2005) [cond-mat/0503393].
- [82] J. Abajo-Arrastia, J. Aparicio and E. Lopez, “Holographic Evolution of Entanglement Entropy,” *JHEP* **1011**, 149 (2010) [arXiv:1006.4090 [hep-th]].
- [83] T. Albash and C. V. Johnson, “Evolution of Holographic Entanglement Entropy after Thermal and Electromagnetic Quenches,” *New J. Phys.* **13**, 045017 (2011) [arXiv:1008.3027 [hep-th]].
- [84] T. Hartman and J. Maldacena, “Time Evolution of Entanglement Entropy from Black Hole Interiors,” *JHEP* **1305**, 014 (2013) [arXiv:1303.1080 [hep-th]].
- [85] H. Liu and S. J. Suh, “Entanglement Tsunami: Universal Scaling in Holographic Thermalization,” *Phys. Rev. Lett.* **112**, 011601 (2014) [arXiv:1305.7244 [hep-th]].
- [86] H. Liu and S. J. Suh, “Entanglement growth during thermalization in holographic systems,” *Phys. Rev. D* **89**, no. 6, 066012 (2014) [arXiv:1311.1200 [hep-th]].
- [87] M. Mezei and D. Stanford, “On entanglement spreading in chaotic systems,” *JHEP* **1705**, 065 (2017) [arXiv:1608.05101 [hep-th]].
- [88] H. Casini, H. Liu and M. Mezei, “Spread of entanglement and causality,” *JHEP* **1607**, 077 (2016) [arXiv:1509.05044 [hep-th]].
- [89] T. Hartman and N. Afkhami-Jeddi, “Speed Limits for Entanglement,” arXiv:1512.02695 [hep-th].
- [90] P. Sabella-Garnier, “Time dependence of entanglement entropy on the fuzzy sphere,” *JHEP* **1708**, 121 (2017) [arXiv:1705.01969 [hep-th]].

- [91] S. Kundu and J. F. Pedraza, “Spread of entanglement for small subsystems in holographic CFTs,” *Phys. Rev. D* **95**, no. 8, 086008 (2017) [arXiv:1602.05934 [hep-th]].
- [92] S. F. Lokhande, G. W. J. Oling and J. F. Pedraza, “Linear response of entanglement entropy from holography,” *JHEP* **1710**, 104 (2017) [arXiv:1705.10324 [hep-th]].
- [93] Y. O. Nakagawa, G. Sroši and T. Ugajin, “Chaos and relative entropy,” *JHEP* **1807**, 002 (2018) doi:10.1007/JHEP07(2018)002 [arXiv:1805.01051 [hep-th]].
- [94] J. M. Magn, “Black holes, complexity and quantum chaos,” *JHEP* **1809**, 043 (2018) doi:10.1007/JHEP09(2018)043 [arXiv:1805.05839 [hep-th]].
- [95] S. A. Hosseini Mansoori and M. M. Qaemqaqami, “Complexity Growth, Butterfly Velocity and Black hole Thermodynamics,” arXiv:1711.09749 [hep-th].
- [96] M. Blake, “Universal Charge Diffusion and the Butterfly Effect in Holographic Theories,” *Phys. Rev. Lett.* **117**, no. 9, 091601 (2016) [arXiv:1603.08510 [hep-th]].
- [97] M. Blake, “Universal Diffusion in Incoherent Black Holes,” *Phys. Rev. D* **94**, no. 8, 086014 (2016) [arXiv:1604.01754 [hep-th]].
- [98] R. A. Davison, W. Fu, A. Georges, Y. Gu, K. Jensen and S. Sachdev, “Thermoelectric transport in disordered metals without quasiparticles: The Sachdev-Ye-Kitaev models and holography,” *Phys. Rev. B* **95**, no. 15, 155131 (2017) [arXiv:1612.00849 [cond-mat.str-el]].
- [99] M. Blake, R. A. Davison and S. Sachdev, “Thermal diffusivity and chaos in metals without quasiparticles,” *Phys. Rev. D* **96**, no. 10, 106008 (2017) [arXiv:1705.07896 [hep-th]].
- [100] S. Grozdanov, K. Schalm and V. Scopelliti, “Black hole scrambling from hydrodynamics,” *Phys. Rev. Lett.* **120**, no. 23, 231601 (2018) [arXiv:1710.00921 [hep-th]].
- [101] M. Blake, H. Lee and H. Liu, “A quantum hydrodynamical description for scrambling and many-body chaos,” arXiv:1801.00010 [hep-th].
- [102] S. Grozdanov, K. Schalm and V. Scopelliti, “Kinetic theory for classical and quantum many-body chaos,” arXiv:1804.09182 [hep-th].
- [103] M. Blake, R. A. Davison, S. Grozdanov and H. Liu, “Many-body chaos and energy dynamics in holography,” *JHEP* **1810**, 035 (2018) doi:10.1007/JHEP10(2018)035 [arXiv:1809.01169 [hep-th]].
- [104] F. M. Haehl and M. Rozali, “Effective Field Theory for Chaotic CFTs,” *JHEP* **1810**, 118 (2018) doi:10.1007/JHEP10(2018)118 [arXiv:1808.02898 [hep-th]].

- [105] S. Sachdev and K. Damle “Non-zero temperature transport near quantum critical point” *Phys. Rev. B* **56**, 8714 (1997). [arXiv:cond-mat/9705206]
- [106] S. Sachdev, “Quantum phase transitions,” Cambridge University Press (1999)
- [107] S. A. Hartnoll, “Theory of universal incoherent metallic transport,” *Nature Phys.* **11**, 54 (2015) doi:10.1038/nphys3174 [arXiv:1405.3651 [cond-mat.str-el]].
- [108] A. Lucas and J. Steinberg, “Charge diffusion and the butterfly effect in striped holographic matter,” *JHEP* **1610**, 143 (2016) doi:10.1007/JHEP10(2016)143 [arXiv:1608.03286 [hep-th]].
- [109] R. A. Davison, W. Fu, A. Georges, Y. Gu, K. Jensen and S. Sachdev, “Thermoelectric transport in disordered metals without quasiparticles: The Sachdev-Ye-Kitaev models and holography,” *Phys. Rev. B* **95**, no. 15, 155131 (2017) doi:10.1103/PhysRevB.95.155131 [arXiv:1612.00849 [cond-mat.str-el]].
- [110] M. Baggioli, B. Goutraux, E. Kiritsis and W. J. Li, “Higher derivative corrections to incoherent metallic transport in holography,” *JHEP* **1703**, 170 (2017) doi:10.1007/JHEP03(2017)170 [arXiv:1612.05500 [hep-th]].
- [111] K. Y. Kim and C. Niu, “Diffusion and Butterfly Velocity at Finite Density,” *JHEP* **1706**, 030 (2017) doi:10.1007/JHEP06(2017)030 [arXiv:1704.00947 [hep-th]].
- [112] A. Mokhtari, S. A. Hosseini Mansoori and K. Bitaghsir Fadafan, “Diffusivities bounds in the presence of Weyl corrections,” *Phys. Lett. B* **785**, 591 (2018) doi:10.1016/j.physletb.2018.09.020 [arXiv:1710.03738 [hep-th]].
- [113] M. Blake, R. A. Davison and S. Sachdev, “Thermal diffusivity and chaos in metals without quasiparticles,” *Phys. Rev. D* **96**, no. 10, 106008 (2017) doi:10.1103/PhysRevD.96.106008 [arXiv:1705.07896 [hep-th]].
- [114] D. Ahn, Y. Ahn, H. S. Jeong, K. Y. Kim, W. J. Li and C. Niu, “Thermal diffusivity and butterfly velocity in anisotropic Q-Lattice models,” arXiv:1708.08822 [hep-th].
- [115] B. Swingle, “Unscrambling the physics of out-of-time-order correlators”, *Nature Physics*, **14**, 988990 (2018)
- [116] J. S. Cotler *et al.*, “Black Holes and Random Matrices,” *JHEP* **1705**, 118 (2017) Erratum: [JHEP **1809**, 002 (2018)] doi:10.1007/JHEP09(2018)002, 10.1007/JHEP05(2017)118 [arXiv:1611.04650 [hep-th]].
- [117] A. M. García-García and J. J. M. Verbaarschot, “Spectral and thermodynamic properties of the Sachdev-Ye-Kitaev model,” *Phys. Rev. D* **94**, no. 12, 126010 (2016) doi:10.1103/PhysRevD.94.126010 [arXiv:1610.03816 [hep-th]].

- [118] A. M. García-García and J. J. M. Verbaarschot, “Analytical Spectral Density of the Sachdev-Ye-Kitaev Model at finite N,” Phys. Rev. D **96**, no. 6, 066012 (2017) doi:10.1103/PhysRevD.96.066012 [arXiv:1701.06593 [hep-th]].
- [119] P. Saad, S. H. Shenker and D. Stanford, “A semiclassical ramp in SYK and in gravity,” arXiv:1806.06840 [hep-th].